View metadata, citation and similar papers at core.ac.uk

brought to you by CORE

provided by Illinois Digital Environment for Access to Learning and Scholarship Repository

MODELING AND SIMULATION OF COMMERCIAL AIRCRAFT ELECTRICAL SYSTEMS

BY

CHRISTOPHER MAK

THESIS

Submitted in partial fulfillment of the requirements
for the degree of Master of Science in Electrical and Computer Engineering
in the Graduate College of the
University of Illinois at Urbana-Champaign, 2015

Urbana, Illinois

Adviser:

Professor Philip T. Krein

ABSTRACT

In this thesis a modeling and simulation based methodology is proposed to study the general power flow and dynamics of commercial aircraft electrical systems. This was done by creating a toolset composed of the crucial elements to model an aircraft electrical system that consists of power sources, power conversion, power distribution, and electrical loads. The considerations for the component models were modularity, computation time, accuracy, ease of use, and an integration with other aircraft system components. The individual components were modeled to be interchangeable and interface with the other components. Several techniques were used to simplify each component model and reduce the computational resources while still maintaining the component dynamic behavior and interactions. A MATLAB/Simulink platform was used to build the components because it is a resource available to others. An average model approach was used for some of the components because the "fast" dynamics will appear as transients to the other aircraft systems like the thermal system.

The component models were used to model and simulate the electrical system in faster than real time for a real mission. The sample aircraft architecture that was modeled was that of the Boeing 737, a typical twin-engine aircraft. Aside from the components that were modeled, the various simulations were performed using a sample flight profile of an aircraft, which details parameters of flight over time, and an engine model developed in Numerical Propulsion System Simulation (NPSS). The following scenarios were simulated: no fault or failure, temporary disconnection between generator and load, and single-generator failure. All of the simulations were conducted using a similar flight profile with small adjustments for the single-generator failure scenario.

ACKNOWLEDGMENTS

This work was supported by Rolls-Royce, Inc. There are many people to thank who helped this project and helped me grow as a person and engineer. I would like to first thank Robert W. Cedoz and Keith D. Noderer from Rolls-Royce for leading this project.

I would like to give special thanks to my advisor, Professor Philip T. Krein, for his support, knowledge, guidance, and patience. I will forever be thankful for this tremendous opportunity he has given me.

Furthermore, I would like to thank Professors Andrew G. Alleyne and Anthony M. Jacobi from the UIUC Department of Mechanical and Industrial Engineering, and Professor Steven J. D'Urso from the UIUC Department of Aerospace Engineering, for their expertise and guidance on this project. Their knowledge and advice have helped improve this project.

I would like to thank my fellow UIUC Power and Energy Systems graduate students. I would like to especially thank Dr. Srikanthan Sridharan and Dr. Veysel Tutku Buyukdegirmenci, who helped compose the various electrical component blocks. A few other UIUC graduate students who assisted in this project are Matthew Williams, Subhabrata Banerjee, Craig Pauga, and Zachary Herman.

Finally, I could never have arrived here without my amazing family. I would love to give thanks to my father Dennis Mak, and brothers Timothy Mak and Jonathan Mak, for their love, support, and sacrifice. Finally, everything I do and achieve is in loving memory of my mother, Fannie Mak, who sacrificed everything for her family.

Table of Contents

1 INTRODUCTION

1.1 Background and Motivation

Every day, tens of thousands of flights deliver people all across the world. With that many flights per day, improvements to fuel efficiency and reductions of emissions are a constant focus and challenge in designing future aircraft. The development of more-electric and an all-electric aircraft (MEA and AEA) is a step in the evolution of more efficient aircraft. For an MEA and AEA, many of the components in thermal, pneumatic and hydraulic systems are replaced with electrically driven ones. These future aircraft require new approaches to design and development

The design and development of an aircraft is an arduous process that can take many years. Early on, in the definition phase (after the concept phase) when the requirements are being defined, complex aircraft systems are separated to minimize the interface complexity between systems while maintaining a complete system view to ensure that design requirements are met [1]. This approach is not optimal as individual models for each sub-system are created and interface parameters between systems are negotiated between different groups [2]. This approach to systems design is outdated. For an MEA architecture as many of the components are replaced with electrically driven components, the divide between systems becomes obscured as sub-systems become more integrated and more complex. Thus separating these sub-systems becomes difficult and important interfaces can be lost. Therefore, a more integrated approach to the definition process is needed.

The development of modeling and simulation tools has greatly assisted the design of aircraft structures, flight control, and aircraft systems. Modeling and simulation tools have been used to model standalone commercial aircraft electrical systems as in [3], [4], and [5]. Modeling

and simulation tools that include the integration and energy flow between sub-systems have been recently developed [6], [7]. This thesis details the development of a user-friendly MATLAB/Simulink based toolset to model and simulate commercial aircraft electrical systems with a primary focus on analyzing power and energy flow over an entire flight. This toolset is part of a larger power flow analysis toolset that allows the modeling of thermal, hydraulic, and other systems. Portions of this work appear in [8].

One of the key challenges to an integrated modeling and simulation approach is that the dynamics for each aircraft system operate at different time scales. The thermal system tends to operate on a "slow" time scale, while the electrical system tends to operate on a "fast" time scale. The quick transient dynamics of the "fast" electrical system will not be noticed in the slow time scale of the thermal system. Keeping this integration in mind, component models are initially designed as simplified (through linearization or reduction of order) models that capture basic dynamics or as an averaged model with little detail. More detailed component models will take up more computational resources and may not affect the interface between electrical and thermal systems. More detailed component models will be added for users who desire it.

The toolset is modular in approach to support the evaluation of various architectures including future MEA architectures. As a point of comparison and to establish confidence in the approach for application to future components, the Boeing 737 architecture was modeled and simulated under various conditions. The Boeing 737 is a typical twin-engine aircraft commonly used in air travel with plenty of documentation [9], [10], [11], [12].

1.2 Thesis Outline

This thesis is focused on the power flow toolset based on fast simulation to analyze hours of flight and to be integrated with other aircraft systems like the thermal system, which operates at a slower time scale. The toolset is designed to be modular, scalable, and easy to use. Individual components of the electrical system were built. Each component has a property menu in which various properties can be changed. This toolset can be integrated with a more complete overview of an aircraft [8] to evaluate the power flow through different sub-systems of the aircraft.

The complete toolset includes components from the thermal, hydraulic, electrical, and mechanical sub-systems traditionally found on commercial aircraft. This toolset is an integrated modeling tool for design that captures the power flow through and between the various sub-system. Various aspects of operation and design such as component sizing, energy requirements, sub-system-level losses, and fault conditions can be analyzed.

In Chapter 2, the general overview of the electrical system is discussed. In Chapter 3, the various electrical components that have been modeled are discussed. First, each component model is shown with its various inputs and outputs. Next, the user interface (property menu) is presented, in which the component may be scaled. Finally, the approach and component mathematical models are discussed. The components that are described can be split into power sources, power conversion, and electrical loads. The main power source is the synchronous generators detailed in [13], [14], [15], while the other power source is the battery that can be modeled using either an electrochemical approach [16], [17] or an electrical circuit approach [18]. The power conversion components include transformers, rectifiers, and inverters [19] found in [20]. Most of these component models are assumed to be lossless, but additional switch loss

models presented in [21] can be used. In Chapter 4, various simulations are presented. Each simulation is based on a sample flight profile. In Chapter 5, conclusions and future work are discussed.

2 SYSTEM OVERVIEW

2.1 Aircraft Electrical System Overview

The electrical system for a commercial aircraft is a complex mix of ac components and dc components intended to form a reliable and redundant system. The electrical system can be divided into four sections: power sources, power distribution, power conversion, and electrical loads. Power comes from the generators and battery. The generators take power from the engines through a gearbox. Power is then distributed by the ac and dc buses. Power is converted by the transformers, inverters, and rectifiers. Power is consumed by the electrical loads to do work or provide other functions.

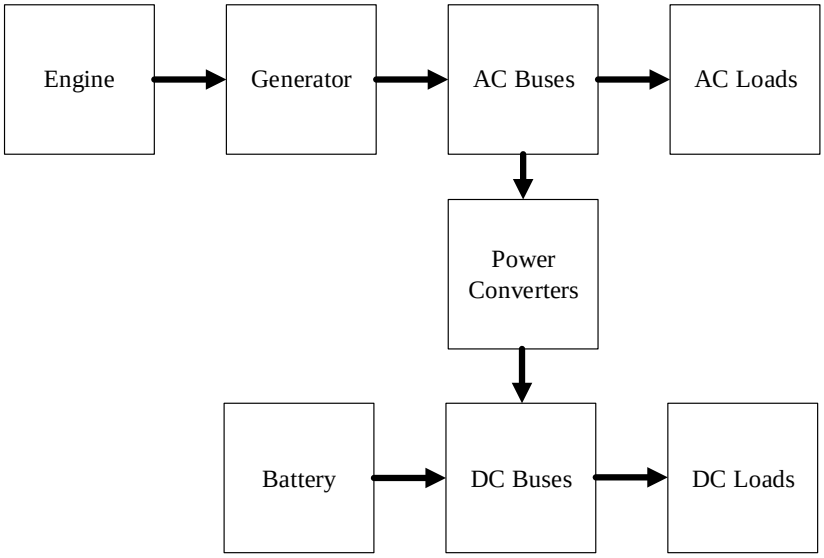

Figure 1: Typically aircraft power flow overview

Figure 1 illustrates the power flow through an aircraft electrical system configuration for an aircraft. The generators convert mechanical energy from the engines. The generators deliver power to several ac buses that distribute the power to the various ac loads and to the power converters. The power converters convert the power to dc and deliver it to the dc bus so the generators can power dc loads. The battery is also connected to the dc bus and provides power to the dc loads.

2.2 Aircraft Electrical System Simulink Model Overview

One of the goals in designing and developing this toolset is to make it available and user-friendly. The MATLAB/Simulink environment was chosen because of its availability and its capability. It has a wide user base that spans students to professional engineers. It allows the creation of graphical overlays, warnings, and help files for each component model, which are intended to help guide the user in making a model and running a successful simulation. In most of the component models, a property menu can be accessed where various parameters of the component can be specified to scale the component to the user's needs.

MATLAB/Simulink is a block diagram environment where each block interfaces and communicates variables with other blocks through signal lines. The variables are usually physical quantities such as voltage, temperature, pressure, etc. Simulink blocks can have inputs that receive signal lines and outputs that send signal lines. Through MATLAB/Simulink's graphical editor it is straightforward to see the flow of variables between blocks.

The input to the electrical system as a whole is shaft speed from the engines. The outputs of the electrical system as a whole are shaft torque sent back to the engines and power loss from different components sent to the environment control system (ECS) or other thermal management systems [8]. The mechanical power of the engine is the shaft torque times the shaft speed. Within the electrical system, the only physical quantities being transferred between the various component models are ac voltage, ac current, dc voltage, and dc current.

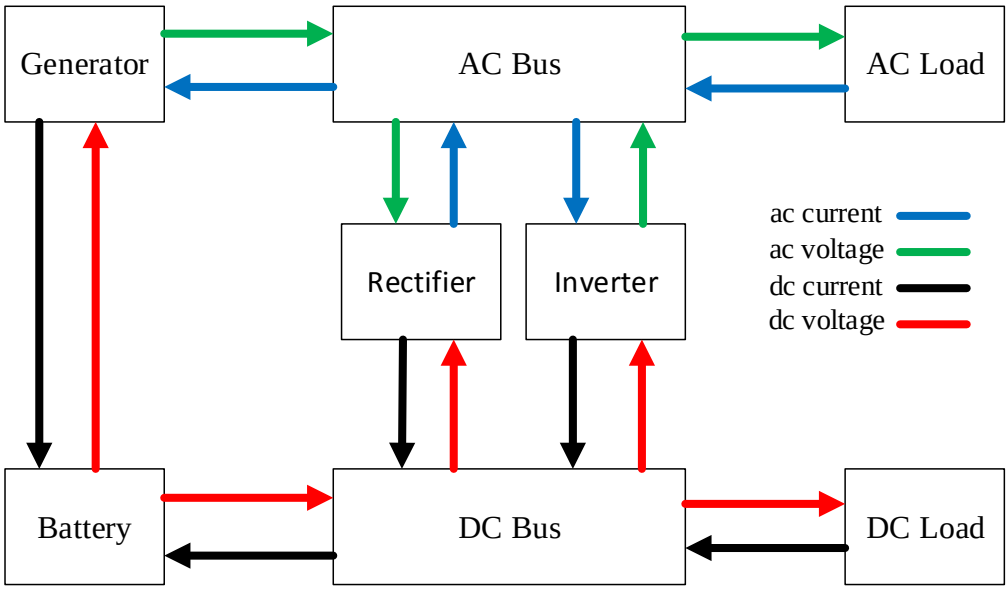

Figure 2: Internal electrical system Simulink overview

Figure 2 illustrates the signal lines or physical quantities being sent between components and the loops that are formed. The generator and battery provide a voltage signal and take in a current signal. Opposite of that, the electrical loads provide a current signal and take in a voltage signal. The buses in between transfer both of these signals. The rectifier and inverter convert the signals to different forms. For this model, the battery provides the exciter generator with field excitation as will be described later. The battery imposes a dc current on the generator and the generator imposes a dc voltage on the battery. The power of the various electrical components can be calculated by multiplying the voltage by the current. The resistance and self-impedances in the wiring between components have been neglected.

Each bus is uniquely defined with different structures to account for different conditions. Since the buses are used for directing the voltage and current signals to the appropriate positions, Simulink switches and comparators are used. The bus models can be seen in the Appendix.

Figure 2 also illustrates that there are many loops of variables between electrical components. These physical loops can give rise to algebraic loops in the Simulink model.

Algebraic loops represent equations that rely on information about the current state to solve the current state. An example of such equations is

$$x(t) = f\left(x(t), t\right) \tag{1}$$

The issues with algebraic loops are simulations that may not start due to unknown initial conditions, simulations that will fail to converge, simulations that will take a long time to solve, or simulations that give rise to singularities. One technique to mitigate algebraic loops is to impose dynamics, attempting to create a causal result in place of (1). This can be done by adding a delay throughout each loop. The delay breaks (1) into a discrete equation with a predefined initial condition such as

$$x(t + \Delta t) = f\left(x(t), t\right) \tag{2}$$

Equation (2) avoids implicit loops compared to (1). This is done through memory blocks that are continuous unit delays where the sampling is continuous. However, the delays can impose artificial dynamic instabilities.

Another technique for circumventing the algebraic loops is to break them. From the modular approach, the user can provide an input to any component model. For example, the loop between the generator and battery can be broken by defining the voltage into the generator. This can be done if the battery voltage is assumed to be constant. Instead of the loop, the generator just imposes a dc current demand on the battery. This can be done for various algebraic loops.

A third method is to reduce algebraic loops, solving (1) a priori and using only the final result. However, this is not a useful approach for large-scale modular simulations.

3 COMPONENT MODELING

3.1 Synchronous Generator

On an aircraft, all of the electrical loads are powered by the generators. On modern commercial aircraft, synchronous generators are most common [9]. The approach for the generator model starts by considering the revolving field circuit in a synchronous machine being driven by an engine [13]. The synchronous generator model is based on voltage output and load information is used to compute the open-circuit line voltage. A singular perturbation approach presented in literature [14] is followed to optimize the system model details and simulation speed. This is appropriate because there are few generators on an aircraft and the electrical loads are lumped together.

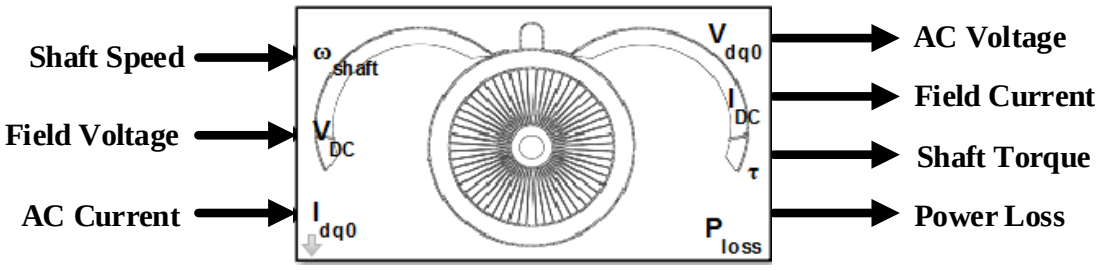

Figure 3: Synchronous generator block model with inputs and outputs

The inputs to the generator model shown in Figure 3 are

- ω - Shaft speed from the engine (RPM)
- V_{fd} - Field voltage from the battery (V)
- i_{dq0} - Synchronous reference frame line currents from the ac loads (A)

The outputs from the generator model are

- v_{dq0} - Synchronous reference frame line voltages delivered to the ac buses or loads (V)
- i_{fd} - Field current delivered to the battery (A)

- T_{em} - Electromagnetic torque imposed on the engine (N-m)
- P_{loss} - Power loss as heat rejected to the cooling system or ambient (W)

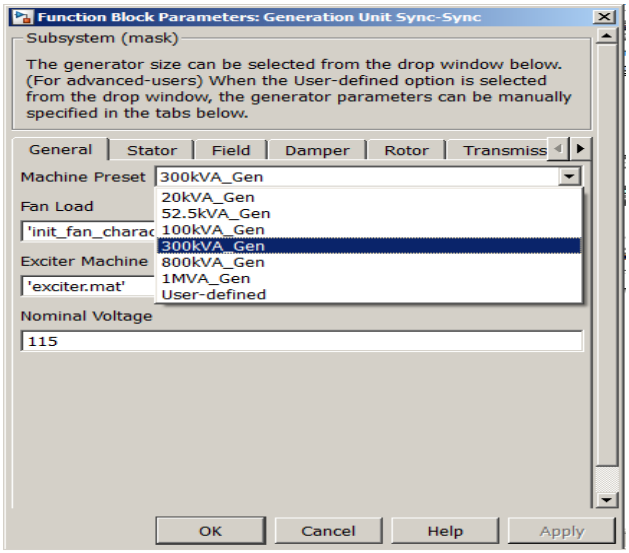

Figure 4: Synchronous generator property menu

The initial parameters from the property menu as seen in Figure 4 that can be defined are

- ***Machine Preset*** - Select various sized generators or customize generator
- ***Fan load*** - Define load fan characteristics
- ***Exciter Machine Parameters*** - Define the exciter generator characteristics
- V_{nom} - The nominal voltage of the generator (V)

From the ***Machine Preset***, the parameters that characterize each generator, mentioned in the generator property menu, are automatically loaded as one of the options is selected. The parameters are taken from the synchronous machine model from the Matlab Simscape library that are obtained by observing responses at the machine terminals with suitable tests scenarios [22]. These Simscape library models are not used for this toolset because they are not suitable for faster than real-time simulations. The various parameters can be seen but not changed through the tabs. However, when the "User-defined" option is selected from the drop-down menu, the

parameters in the other tabs can be changed as seen in Figure 5, allowing the user to characterize a generator outside of the preselected options. These user-characterized generators may result in system instability and non-convergence. The ***Fan load*** parameter is a MAT file that details the rotational speed and load torque characteristics for a cooler fan to the generator. The ***Exciter Machine Parameters*** is a MAT file that characterizes the exciter machine used in the synchronous generator model.

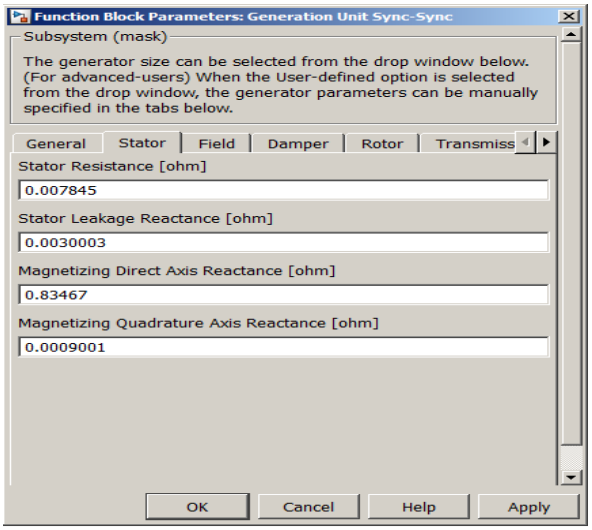

Figure 5: Stator parameter tab of synchronous generator model

The parameters of synchronous generator that can be defined are

- R_s - Stator resistance (Ω)
- X_{ls} - Stator leakage reactance (Ω)
- X_{md} - Magnetizing direct reactance (Ω)
- X_{mq} - Magnetizing quadrature reactance (Ω)
- R_{fd} - Field resistance (Ω)
- X_{lfd} - Field leakage reactance (Ω)
- R'_d - Transient direct axis resistance (Ω)
- X_{l1d} - Transient leakage direct reactance (Ω)
- R'_q - Transient quadrature axis resistance (Ω)
- R_{2q} - Subtransient quadrature axis resistance (Ω)

- X_{l1q} - Transient leakage quadrature axis reactance (Ω)
- X_{l2q} - Subtransient leakage quadrature axis reactance (Ω)
- R_{TL} - Transmission line resistance (Ω)
- X_{TL} - Transmission line reactance (Ω)
- S_{base} - Base complex power (VA)
- V_{BDQ} - Base armature voltage (V)
- ω_{base} - Base electrical frequency (rad/sec)
- P_{base} - Base power (W)

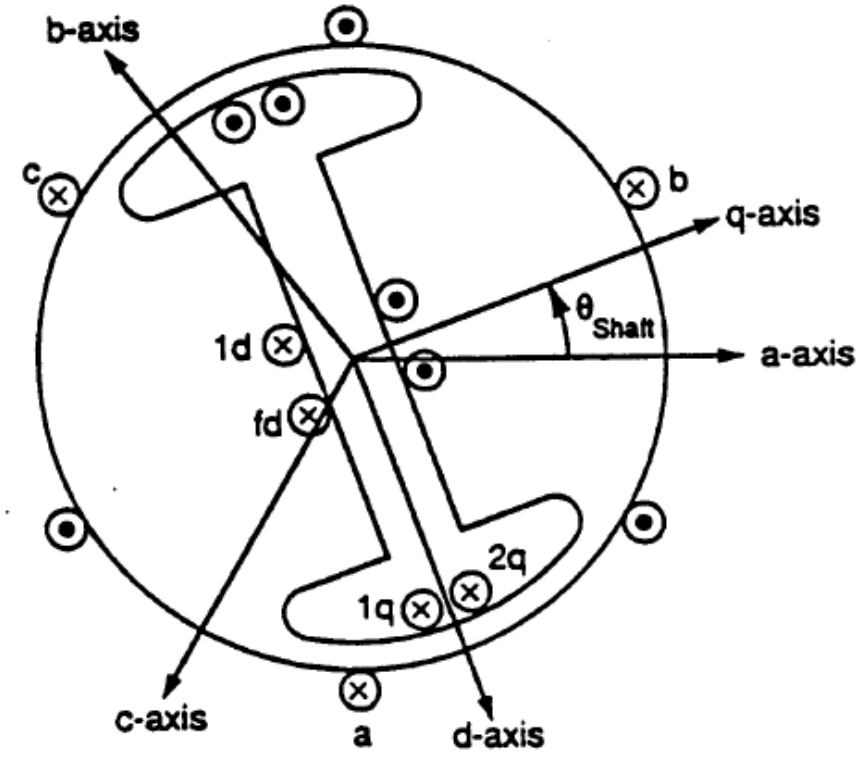

Figure 6: Synchronous machine coil locations and magnetic axes taken from [13]

The synchronous or direct-quadrature-zero (*dq0*) reference frame is employed where the direct and quadrature axes are shown in Figure 6 taken from [14]. The steady states in a balanced symmetrical machine are typically sinusoidal, which are computationally intensive. These sinusoidal states are transformed (using Park's transformation [14]) to constant states in the *dq0* reference frame, resulting in simpler calculations and faster simulations. Also, the dynamics

equations are simplified. Therefore, all of the ac voltages and ac currents throughout the electrical system are defined in the *dq0* reference frame.

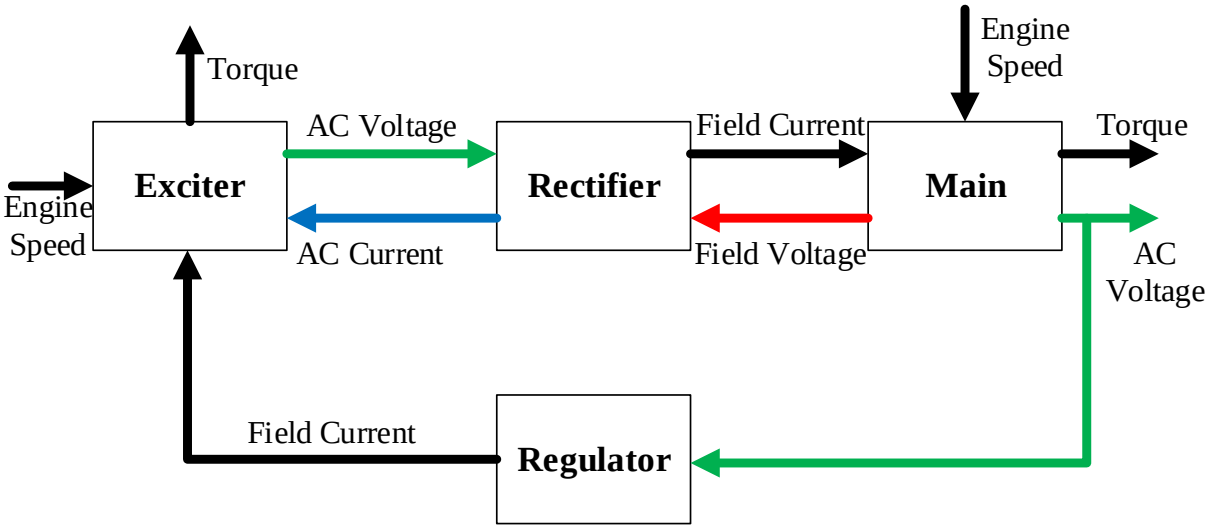

Figure 7: Synchronous generator component model overview

The synchronous generator is made up of different components as shown in Figure 7 that will be discussed in the following sections. The different components that make up the synchronous generator model are the synchronous machines (main generator and exciter generator), rectifier, and the controller. The Simulink model of the synchronous generator can be seen in Appendix A.

3.1.1 Exciter Generator

The main generator requires a direct field current supply for excitation of its magnetic field. Commonly, another wound-field or permanent magnet synchronous generator coupled to the main generator is utilized to provide this current [15]. The field current must be provided independent of the generator through an active rectifier and must be controlled properly to regulate the generator terminal voltage. The Simulink model of the synchronous machine can be seen in Figure 8 with its various inputs and outputs.

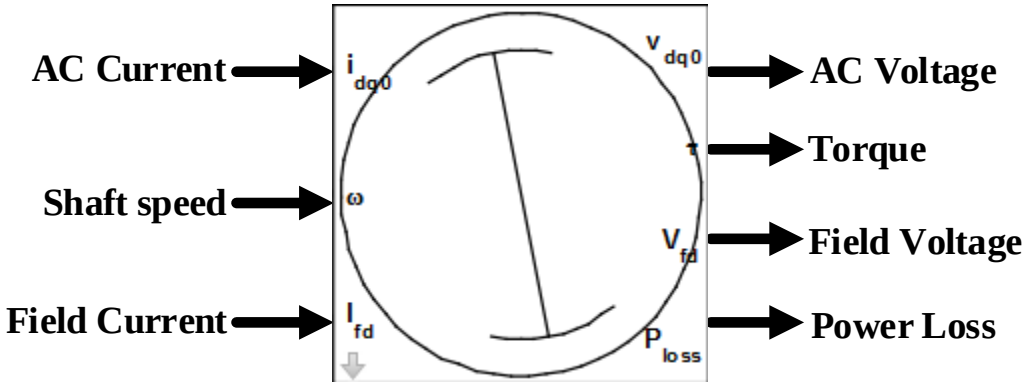

Figure 8: Synchronous machine block model with inputs and outputs

Similar to the synchronous generator, the inputs to the synchronous machine are

- $\boldsymbol{i_{dq0}}$ - Synchronous reference frame line current from loads (for the generator machine) or from the synchronous generator rectifier (for the exciter machine) (A)
- $\boldsymbol{\omega}$ - Rotational shaft speed from the engine (rad/s)
- $\boldsymbol{i_{fd}}$ - Field current from the synchronous generator rectifier (for the generator machine) or from the dc-dc converter (for the exciter machine) (A)

The outputs to the synchronous machine are

- $\boldsymbol{v_{dq0}}$ - Synchronous reference frame line voltages sent as an output (for the generator machine) or imposed to rectifier (for the exciter machine) (V)
- $\boldsymbol{T_{em}}$ - Electromagnetic torque sent as an output (N-m)
- $\boldsymbol{V_{fd}}$ - Field voltage imposed on the rectifier for the generator machine (V)
- $\boldsymbol{P_{loss}}$ - Power loss (heat) sent as an output (W)

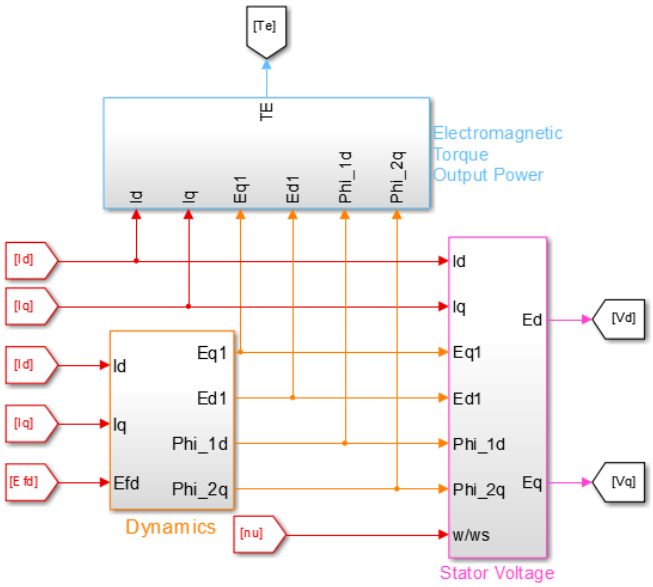

Figure 9: Synchronous machine block diagram

The following equations for calculating voltages and torque are taken from [14]. Several variables are defined and converted to their per unit equivalent as can be seen in Appendix B. The direct and quadrature axis transient electromotive forces, $E_q^{'}$ and $E_d^{'}$ respectively, are defined by their flux linkage (ψ) and current (I_d and I_q) relationship. By using transient field winding time constants ($T_{do}^{'}$ and $T_{qo}^{'}$), subtransient time constants ($T_{do}^{''}$ and $T_{qo}^{''}$), transient reactances ($X_d^{'}$ and $X_q^{'}$), and subtransient reactances ($X_d^{''}$ and $X_q^{''}$), the transient electromotive forces and flux linkages, as seen in the "Dynamics" block in Figure 9, are given by solving the following equations simultaneously:

$$T_{do}^{'}\frac{dE_q^{'}}{dt}=-E_q^{'}-\left(X_d-X_d^{'}\right)\left[I_d-\frac{X_d^{'}-X_d^{''}}{\left(X_d^{'}-X_{ls}\right)^2}\left(\psi_{1d}+\left(X_d^{'}-X_{ls}\right)I_d-E_q^{'}\right)\right]+E_{fd} \tag{3}$$

$$T_{qo}^{'}\frac{dE_d^{'}}{dt}=-E_d^{'}+\left(X_q-X_q^{'}\right)\left[I_q-\frac{X_q^{'}-X_q^{''}}{\left(X_q^{'}-X_{ls}\right)^2}\left(\psi_{2q}+\left(X_q^{'}-X_{ls}\right)I_q+E_d^{'}\right)\right] \tag{4}$$

$$T_{do}^{"}\frac{d\psi_{1d}}{dt}=-\psi_{1d}+E_q^{'}-\left(X_d^{'}-X_{ls}\right)I_d \tag{5}$$

$$T_{qo}^{"}\frac{d\psi_{2q}}{dt}=-\psi_{2q}+E_d^{'}-\left(X_q^{'}-X_{ls}\right)I_q \tag{6}$$

Once the transient electromotive forces and flux linkages are calculated, the direct and quadrature stator voltages (V_d and V_q) are calculated in the "Stator Voltage" block in Figure 9 by using

$$V_q=-\gamma\left(X_d^{"}+X_{TL}\right)I_d-\left(R_s+R_{TL}\right)I_q+\gamma\left(E_q^{'}\frac{X_d^{"}-X_{ls}}{X_d^{'}-X_{ls}}+\psi_{1d}\frac{X_d^{'}-X_d^{"}}{X_d^{'}-X_{ls}}\right) \tag{7}$$

$$V_d=\gamma\left(X_d^{"}+X_{TL}\right)I_q-\left(R_s+R_{TL}\right)I_d+\gamma\left(E_d^{'}\frac{X_q^{"}-X_{ls}}{X_q^{'}-X_{ls}}+\psi_{2q}\frac{X_q^{'}-X_q^{"}}{X_q^{'}-X_{ls}}\right) \tag{8}$$

where γ is the per-unit electrical frequency (typical base value of 377 rad/s). The electromotive torque, (T_{EM}), can be calculated using the subtransient flux linkages by

$$T_{EM}=\left[\left(\frac{X_d^{"}-X_{ls}}{X_d^{'}-X_{ls}}\right)E_q^{'}+\left(\frac{X_d^{'}-X_d^{"}}{X_d^{'}-X_{ls}}\right)\psi_{1d}\right]I_q-\left[\left(\frac{X_q^{"}-X_{ls}}{X_q^{'}-X_{ls}}\right)E_d^{'}+\left(\frac{X_q^{'}-X_q^{"}}{X_q^{'}-X_{ls}}\right)\psi_{2q}\right]I_d+\left(X_q^{''}-X_d^{''}\right)I_dI_q \tag{9}$$

The power loss of the synchronous machines comes from the electrical losses in resistances, magnetic core losses, and mechanical losses from friction. This loss is the difference between the input mechanical power and the output electrical power:

$$P_{loss}=S_B\left(\gamma T_{EM}-E_dI_d-E_qI_q\right) \tag{10}$$

3.1.2 Voltage Regulator and Field Control

The voltage regulator is needed to control the output ac voltages for the main generator to the nominal value, $\boldsymbol{V_{nom}}$, set from the property menu shown in Figure 4. The voltage regulator senses the output voltage, compares it to the nominal voltage and produces a duty ratio that is used by a dc-dc converter. The first part of the voltage regulator compares the output voltage to

the nominal voltage and produces a signal. The controller used in this model determines a duty ratio, $\boldsymbol{D}$, that is sent to a dc-dc converter by

$$V_{line}(t) = \sqrt{V_d^2 + V_q^2} \tag{11}$$

$$\dot{r} = k_1\left(V_{nom} - V_{line}\right) \tag{12}$$

$$\dot{D} = k_2\left(r - k_3 D\right) \tag{13}$$

where $\boldsymbol{k_1}$, $\boldsymbol{k_2}$, and $\boldsymbol{k_3}$ are the controller gains which can be changed

The second part of the voltage regulator is the dc-dc converter that provides field control. A battery provides the exciter generator field current. However, this field current input to the exciter machine is regulated through a dc-dc converter and the controller before the exciter machine. The dc-dc converter is modeled as an ideal, lossless buck converter plus a separate loss block where switch frequency, inductance, capacitance, and equivalent series resistance are not considered. The only information needed by the converter block is the changing duty ratio produced by the voltage controller. This is the lowest level of detail for a converter. However, since the buck converter is only part of the closed loop control used to maintain the output voltage, a detailed model is not necessary and would take up additional computation resources. The buck converter is assumed to only operate in continuous conduction mode as discontinuous conduction mode would change the response and would require additional information such as an additional duty ratio, inductance, and resistances.

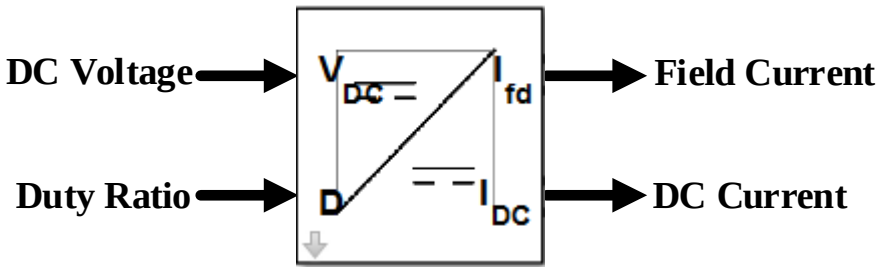

Figure 10: DC-DC converter Simulink block model with inputs and outputs

The inputs to the dc-dc converter model shown in Figure 10 are

- V_{dc} - DC voltage from the battery (V)
- D - Duty ratio from the controller

The outputs to the dc-dc converter are

- I_{fd} - Field current sent to the exciter machine (A)
- I_{dc} - DC battery current sent to the battery (A)

Since duty ratio is defined as a value from zero to one and the duty ratio calculated from Equation (13) can be outside those bounds, the buck converter model initially limits that input from zero to one with lower values bound to zero and higher values bound to one. The field current is calculated by [20]

$$I_{fd} = D \cdot V_{dc} / R_{fd} \tag{14}$$

where R_{fd}, the field resistance, comes from the exciter machine parameters. The output dc battery current is defined as

$$I_{dc} = I_{fd} \times D \tag{15}$$

To capture the conduction and parasitic losses in the buck converter an additional loss model can be used.

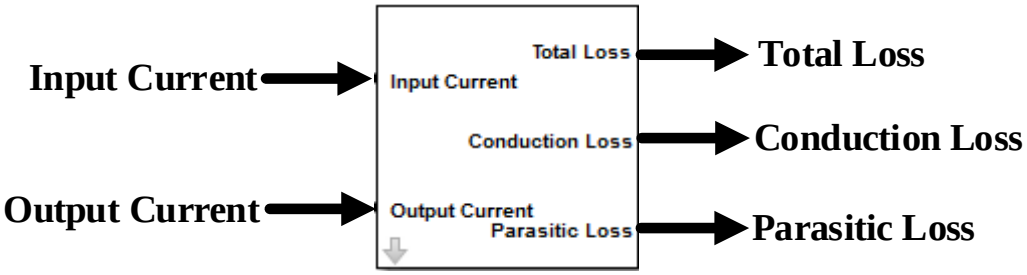

Figure 11: DC-DC Buck converter loss model with inputs and outputs

The inputs to the dc-dc converter loss model as seen in Figure 11 are

- I_{fd} - Field current sent to the exciter machine (A)
- I_{dc} - DC battery current sent to the battery (A)

The outputs to the dc-dc converter loss model are

- P_{tot} - Total power loss (W)
- P_{cond} - Conduction loss (W)
- P_{para} - Parasitic loss (W)

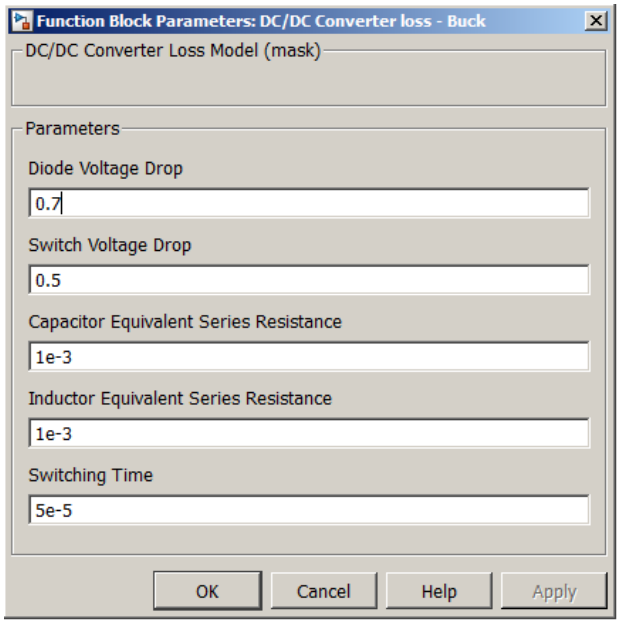

Figure 12: DC-DC buck converter loss model property menu

In the dc-dc buck converter loss model property menu as shown in Figure 12, the following parameters can specified:

- V_{diode} - Diode voltage drop (V)
- V_{sw} - Switching voltage drop (V)
- $ESRC$ - Capacitor equivalent series resistance (Ω)
- $ESRL$ - Inductor equivalent series resistance (Ω)
- DT - Switching time (s)

The conduction losses come from the voltage drops in the diode and the switch and can be defined as

$$P_{cond} = V_{sw} I_{fd} DT + V_{diode} I_{fd} (1 - DT) \tag{16}$$

The parasitic losses come from the equivalent series resistances in the capacitor and inductor components

$$P_{para} = (I_{fd} - I_{DC})^2 ESRC + I_{fd}^2 ESRL \tag{17}$$

The total power loss is the sum of the conduction losses and parasitic losses.

3.1.3 Generator Model Testing

The 100 kVA synchronous generator was tested using constant inputs. Each of the generator's three inputs was tested for its effect on the outputs and for stability. In the first test, the input shaft speed was changed to start the generator with no load current and a constant input voltage of 26 V.

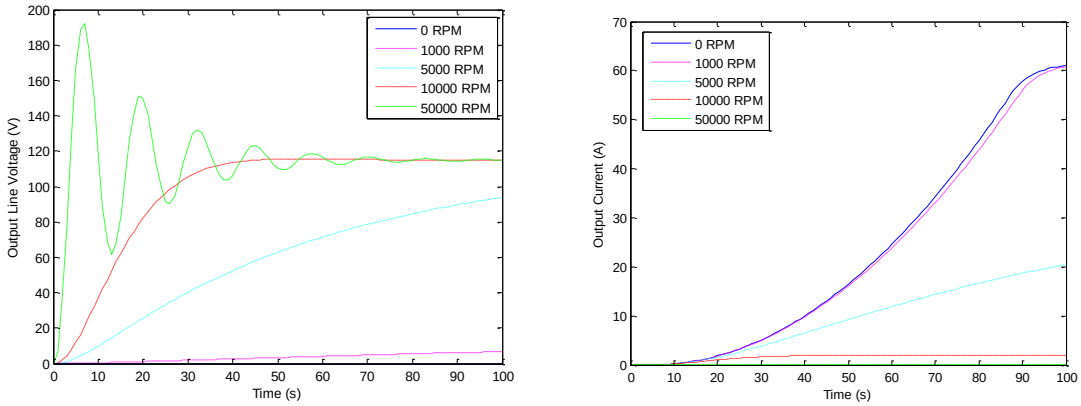

Figure 13: Varying shaft speed test

By varying the shaft speed as shown in Figure 13, it can be seen that with higher values of input shaft speed, the generator will reach its nominal voltage faster but may not necessarily settle to steady state faster because of the limited speed of the voltage controller, resulting in an under-damped harmonic motion. High enough values of shaft speed will cause the voltage in the generator to increase faster than the controller can bring it back to the set nominal value, which will result in an error and crash the generator model. The controller gains can be adjusted and the simulation step size can be reduced to help prevent this error, but these measures only increase the limit before the component model crashes. As for the output field current, as the shaft speed increases the output field current decreases. This result illustrates the over-excitation of the synchronous generator. An increased shaft speed decreases the internal generator voltage and increases the leakage flux, causing the field current to decrease.

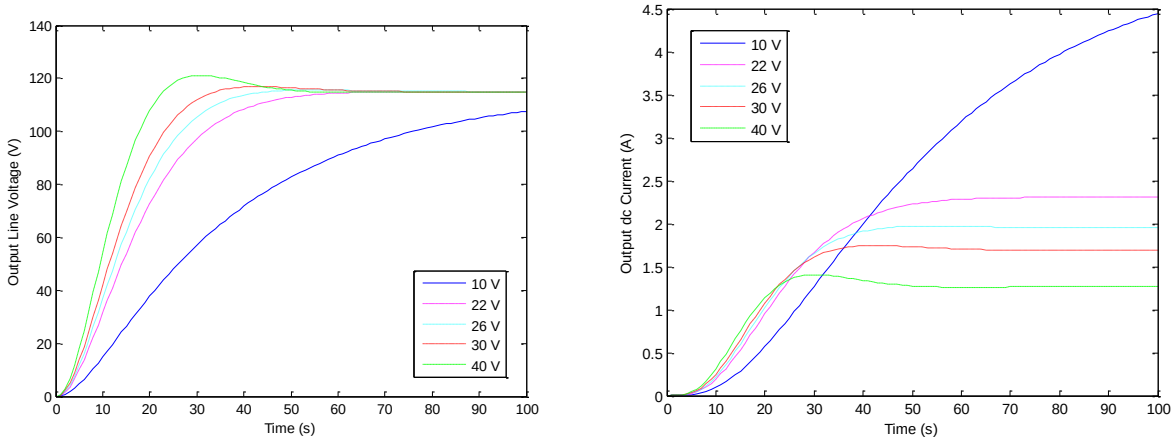

Figure 14: Varying generator input dc voltage

Different input dc voltages were tested while a constant speed of 10000 RPM and no load was used. Figure 14 illustrates that the higher the input dc voltage, the faster the generator voltage will rise, and a lower steady state dc current output will be required. A greater field voltage provides the exciter generator with more power, allowing for a quicker response to steady state.

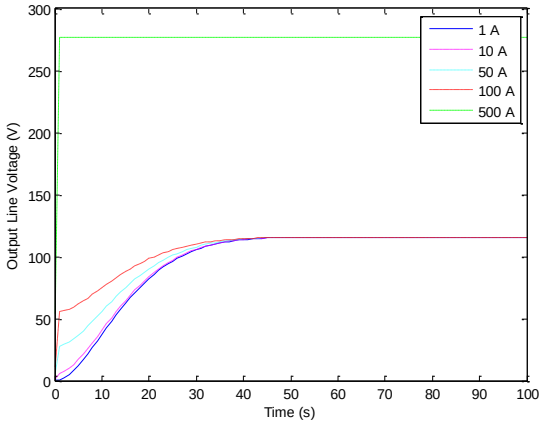

Figure 15: AC voltage waveform to varying line currents for the generator

The final input of the generator model to analyze is the ac current draw from the ac loads. An initial shaft speed of 10000 RPM and input dc voltage of 26 V was used. For the varying initial current loading case shown in Figure 15, high current demands will cause the output

voltage to rise higher. However if the load is too high the generator will settle to a new nominal voltage that is proportional to the load. For a 500 A load the new steady state voltage is 277 V and for a 1000 A load it is 554 V. These results are inconsistent as generators that are overloaded drop voltage and speed. Since the shaft speed and load current are inputs to the component model and held constant, the voltage is forced to a higher steady state to be able to support the load.

3.2 Three-Phase Rectifier

The three-phase rectifier converts the ac voltage to dc voltage. In the synchronous generator, the rectifier is used to provide the dc field current from the exciter generator, which is supported by a battery, to the main generator. This rectifier model is also used in the transformer rectifier unit that will be described later. An active rectifier is used because with passive rectifiers the operating voltage is nonlinear since the batteries and bus capacitors will hold the voltage and no current will flow until the field excitation and speed are sufficient to forward-bias the rectifier bridge. With active rectifiers, an IGBT bridge actively controls the current to present near-unity power factor to the generator.

Full switch-level models are avoided because they are too slow to support analysis of an entire flight. This model does not require information about equivalent series resistance, capacitance, or switching frequency, but inductances are used. The transients are not considered because they happen in a faster time scale that will not be seen by the thermal system. Power factor is assumed to be unity. Power losses in the switches are not considered. Loss model blocks incorporating the losses of the IGBT switches using datasheet information [21] will be added in the future.

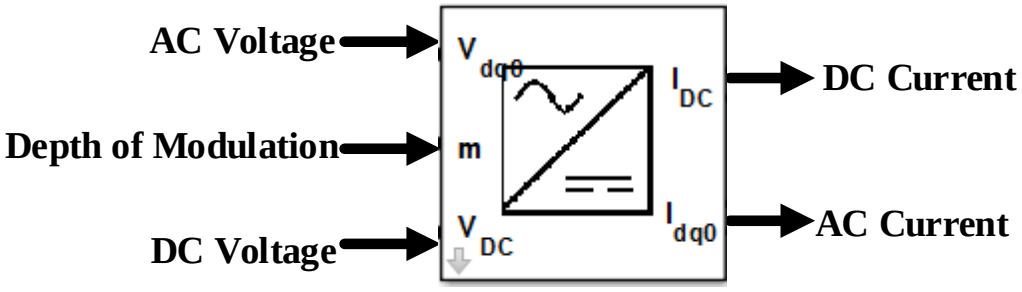

Figure 16: Three-phase active rectifier model with inputs and outputs

The inputs to the three-phase rectifier as seen in Figure 16 are

- V_{dq0} - Synchronous reference frame line voltages from the exciter machine (V)
- m - Depth of modulation that is defined by the user
- V_{DC} - DC field voltage from the generator synchronous machine (V)

The outputs to the three-phase rectifier are

- I_{DC} - DC field current sent to the generator machine (A)
- I_{dq0} - Synchronous reference frame line current sent to the exciter machine (A)

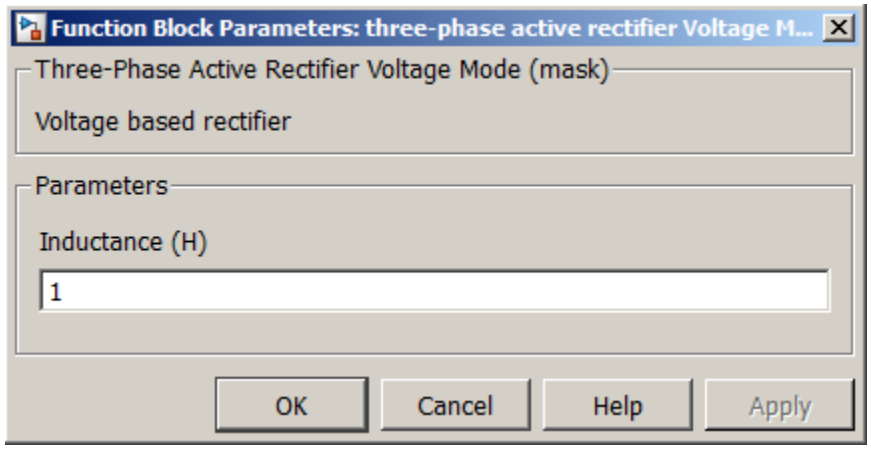

Figure 17: Three-phase active rectifier property menu

In the rectifier property menu seen in Figure 17, the dc-link inductor of the rectifier can be defined. The output dc current from rectifier is given by

$$L\frac{dI_{DC}}{dt} = m \cdot V_{line}(t) - V_{DC} \tag{18}$$

where $V_{line}(t)$ is defined previously in Equation (11) as the norm of the ac voltage. The synchronous reference frame line currents are first determined by the phase angle between the direct and quadrature axes by

$$\theta = \arctan\left(\frac{V_q}{V_d}\right) \tag{19}$$

Using the phase angle, the direct and quadrature line currents are given as

$$i_q = m \cdot i_{DC} \cdot \sin(\theta) \tag{20}$$

$$i_d = m \cdot i_{DC} \cdot \cos(\theta) \tag{21}$$

3.3 Ground Power Supply

The ground power supply is the power supply connected to the aircraft when it is parked on the ground. It is modeled as an unlimited power source that can provide all of the ac current that the aircraft demands while maintaining the nominal voltage. This grid voltage is assumed to be constant and will not change from loading. Since primary focus is on the aircraft power flow and not the aircraft's interaction with the grid, these were not considered.

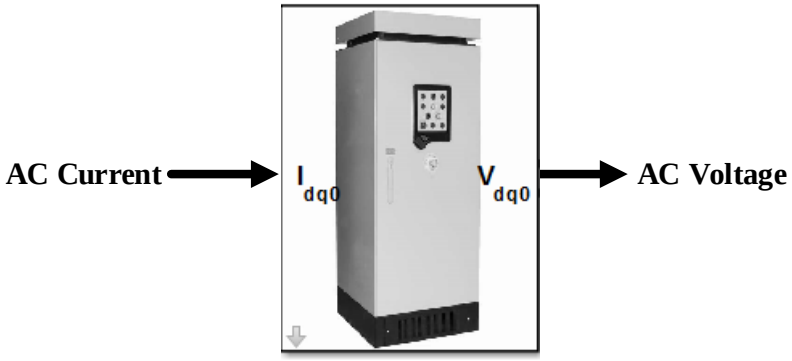

Figure 18: Ground power supply model with inputs and outputs

The input to the ground power supply model as shown in Figure 18 is

- $\boldsymbol{i_{dq0}}$ - Synchronous reference frame line currents from the ac loads (A)

The output to the ground power supply model is

- $\boldsymbol{v}_{dq0}$ - Synchronous reference frame line voltages delivered to the ac buses or ac load (V)

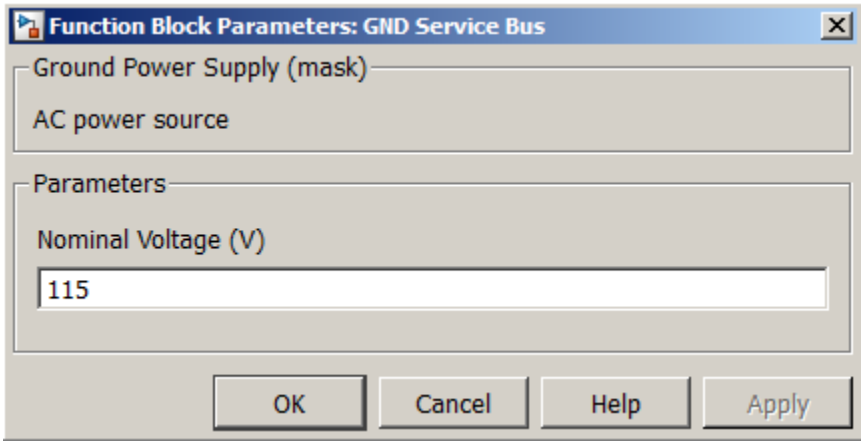

Figure 19: Ground power supply property menu

In the ground power supply property menu shown in Figure 19, the nominal voltage, V_{nom}, can be specified by the user.

3.4 Power Inverter

The power inverter in an aircraft is used to convert the dc voltage of the battery to three-phase ac voltage to supply power to the ac loads in case of emergencies. Pulse-width modulated (PWM) voltage source inverters are used in commercial aircraft [19]. The PWM inverter is modeled as a basic PWM inverter. Voltage and current drops were not used to calculate the output voltage and current as they are small and negligible. The output ac voltage is assumed steady and constant, so no harmonics or high frequency noise were accounted for. An average switching frequency is used and the losses are assumed to be averaged as discussed later.

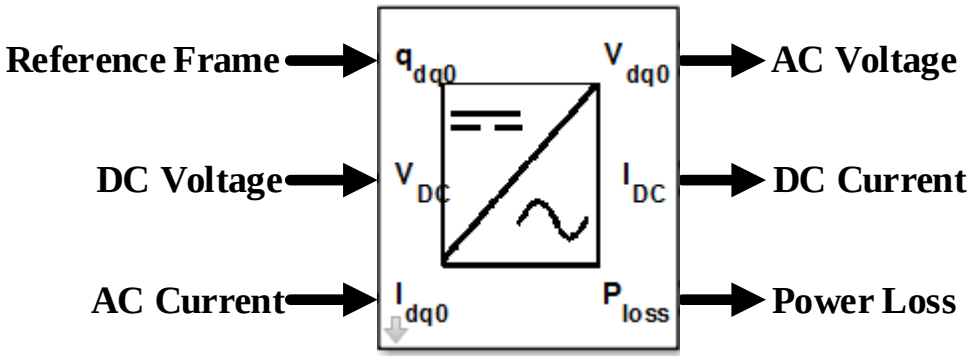

Figure 20: Inverter model with inputs and outputs

The inputs to the inverter model as shown in Figure 20 are

- q_{qd0} - Synchronous reference frame
- V_{dc} - DC voltage from the battery (V)
- i_{dq0} - Synchronous reference frame line current from transformer (A)

The synchronous reference frame is a 1x3 unit vector that describes the reference frame the newly inverted ac voltages will take. The reference frame is defined in the synchronous reference frame phasor block as shown in Figure 21.

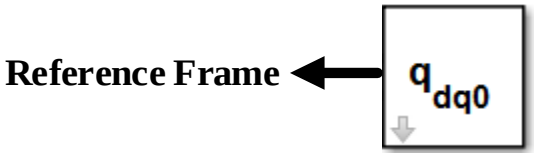

Figure 21: Synchronous reference frame phasor

The outputs to the inverter are

- v_{dq0} - Synchronous reference frame line voltage sent to the transformer (V)
- I_{dc} - DC current sent to the battery (A)
- P_{loss} - Power loss as heat (W)

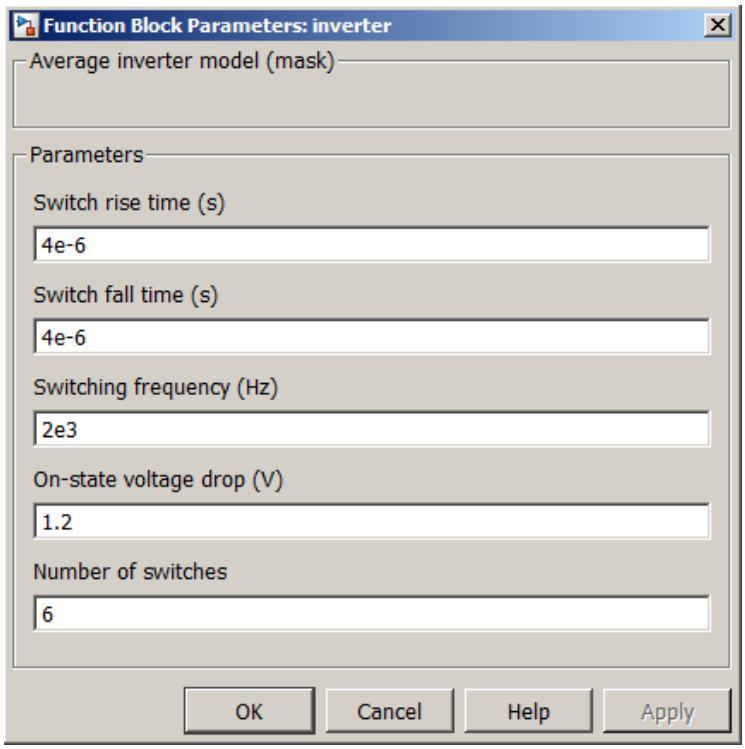

Figure 22: Inverter property menu

In the inverter property menu seen in Figure 22, the following parameters can be specified:

- T_{rise} - Switch rise time of the semiconductor (s)
- T_{fall} - Switch fall time of the semiconductor (s)
- f_{sw} - Switching PWM frequency (Hz)
- V_{on} - On-state voltage drop across the switch during conduction (V)
- N_{sw} - Number of semiconductor switches

For the PWM inverter model, the output ac line voltage and dc current are defined as

$$V_{dq0} = V_{dc} \times q_{dq0} \tag{22}$$

$$I_{dc} = \sum (q_{qd0} \bullet I_{qd0}) \tag{23}$$

The power loss of an inverter comes from the conduction losses and the switching losses [20]. The conduction losses caused by the forward voltage drop of semiconductors are defined as

$$P_{cond} = \left|I_{qd0}\right|_2 \times V_{on} \times N_{sw} \tag{24}$$

The switching losses or computation losses occur during the switching states between on and off. During these states, the transistor voltage is either increasing (transistor turning off) or decreasing (transistor turning on) and the current through the transistor is doing the opposite. By taking the average rise and fall time, the switching loss is defined as

$$P_{sw} = V_{dc} \times \left(\frac{T_{rise} + T_{fall}}{2}\right) \times \left|I_{qd0}\right|_2 \times f_{sw} \times N_{sw} \tag{25}$$

3.5 Transformer

The transformer, typically used in conjunction with the rectifier or inverter on an aircraft, boosts or bucks the ac voltage depending on the number of windings. A steady-state electrical model is implemented where only winding resistances are considered. Inductances, including leakage and mutual inductances, are neglected. Some additional assumptions are that there is no phase shift error in the transformer, no eddy currents, and the transformer is never saturated. The transformer core is loss-free. While a basic transformer model for changing ac voltages was first implemented, a more detailed transformer model will be required as future work to capture the various neglected losses including those losses associated with higher frequency.

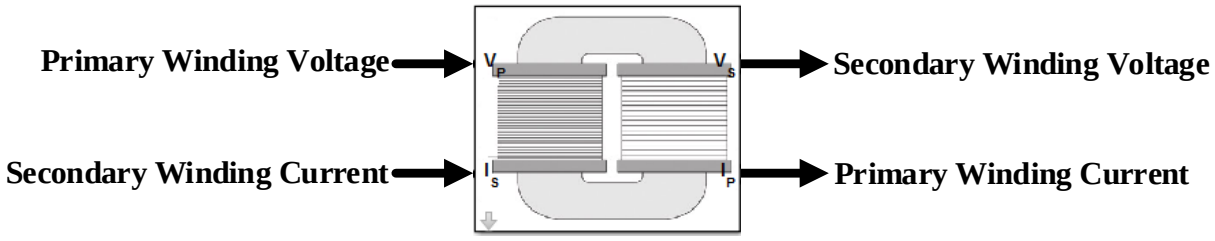

Figure 23: Transformer model with inputs and outputs

The inputs to the transformer model as shown in Figure 23 are

- V_P - Primary winding voltage from the inverter (V)

- I_S - Secondary winding current from the battery (A)

The outputs to the transformer model are

- V_S - Secondary winding voltage sent to the ac bus (V)
- I_P - Primary winding current back to the inverter (A)

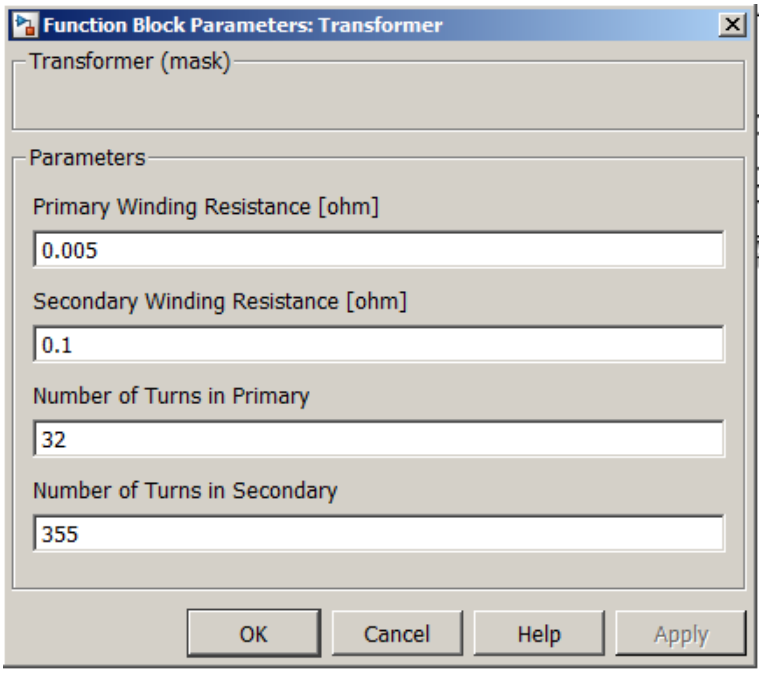

Figure 24: Transformer property menu

In the property menu as seen in Figure 24, the following transformer parameters can be specified:

- R_P - Primary winding resistance (Ω)
- R_S - Secondary winding resistance (Ω)
- N_P - Number of turns in primary winding
- N_S - Number of turns in secondary winding

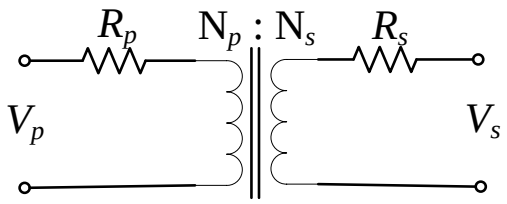

Figure 25: Transformer circuit diagram

In transformer model used, the magnetic coupling was considered ideal and only conduction losses from the windings were considered. Figure 25 illustrates the transformer circuit diagram used to determine the primary winding and secondary winding voltage and current relationships. By using KVL and KCL, these relationships are determined to be

$$\frac{V_P - I_P R_P}{V_S - I_S R_S} = \frac{N_P}{N_S} \tag{26}$$

$$I_P = \frac{N_S}{N_P} I_S \tag{27}$$

3.5.1 Transformer Rectifier Unit

The transformer rectifier unit (TRU) is used to rectify the ac power to charge the batteries and supply power to the dc loads. The TRU is a combination of the transformer model and the rectifier model. It has the same limitations as both component models. The transformer first reduces the input ac voltage that is then used by the rectifier model described previously in Section 3.2.

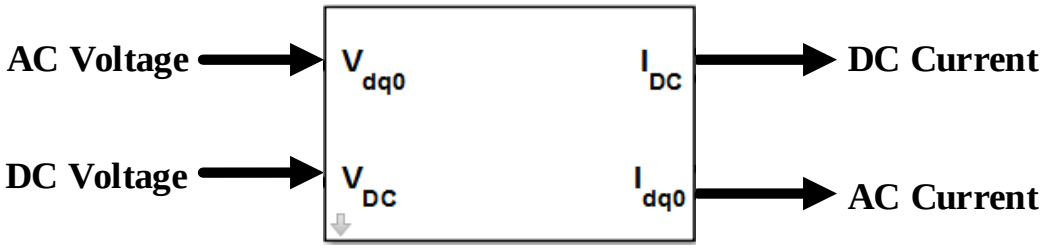

Figure 26: Transformer rectifier unit model with inputs and outputs

The inputs to the transformer rectifier unit as shown in Figure 26 are

- $\boldsymbol{v_{dq0}}$ - Synchronous reference frame line voltages from a generator (V)
- $\boldsymbol{V_{dc}}$ - Output dc voltage from the battery (V)

The outputs to the transformer rectifier unit are

- $\boldsymbol{I_{dc}}$ - Output dc current sent to the battery (A)
- $\boldsymbol{i_{dq0}}$ - Synchronous reference frame line currents sent to a generator (A)

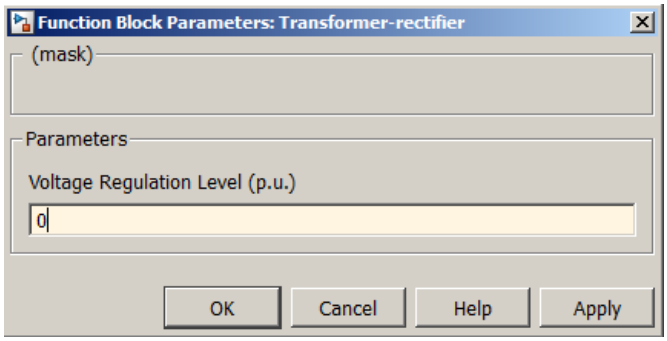

Figure 27: TRU property menu

In the TRU property menu as shown in Figure 27, the voltage regulation level can be adjusted. The purpose of the TRU is to power the dc loads and charge the battery. In the model, the TRU performs both of those tasks simultaneously. This is done by having the battery power all of the dc loads and by having the TRU continuously charge the battery. For an input ac voltage of 115 V, if the battery voltage drops below 28.4 V, the TRU will provide a charging current for the battery as depicted in Figure 28. The TRU will provide more charging current as the battery voltage is lowered. If the battery voltage is above 28.4 V, the TRU will not provide a charging current because the desired dc voltage is more than can be achieved by the rectified ac voltage.

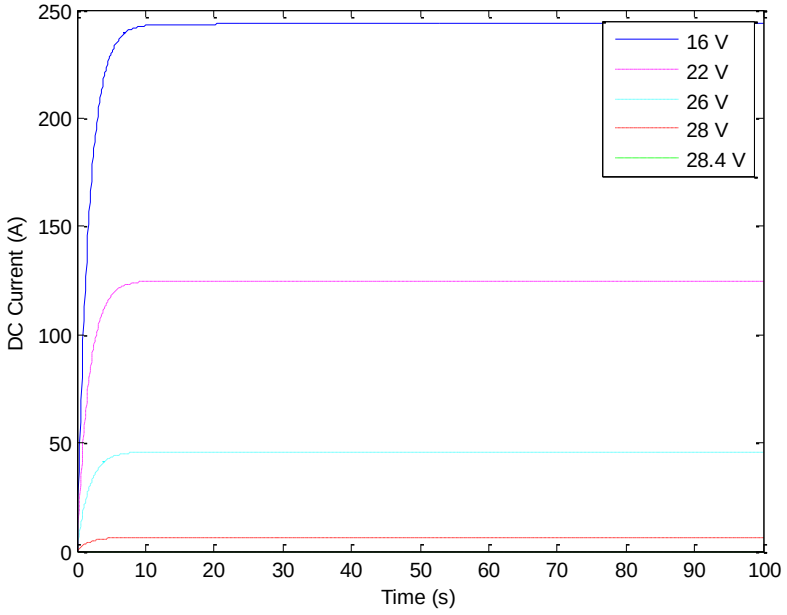

Figure 28: TRU charging rates for v*dq0*=115 V

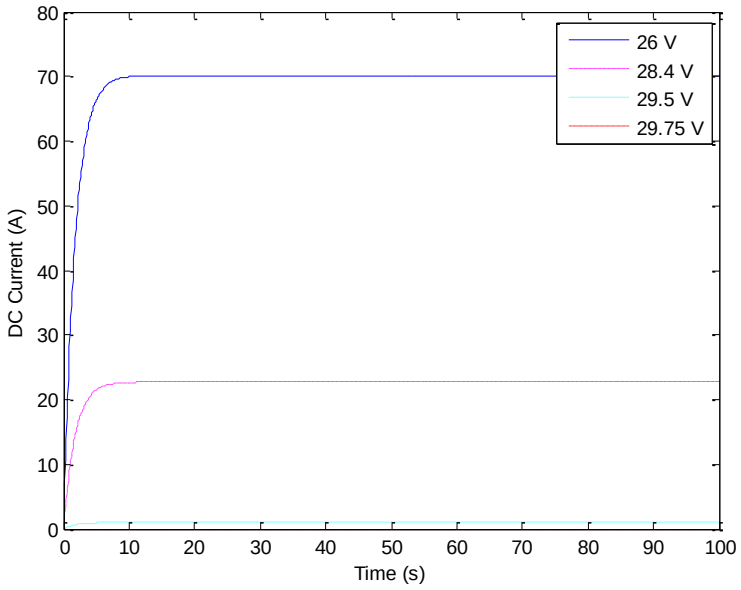

Figure 29: TRU charging rates for v*dq0*=120 V

The 28.4 V limit is not constant because the ac line voltage from the generators will not be constant. When the ac line voltage increases, the battery charging voltage will increase as shown in Figure 29. For an ac line voltage of 120 V, the battery will charge until 29.75 V. When the ac

line voltage increases, the charging current also increases. By comparing the 26 V waveforms for both cases in Figure 28 and Figure 29, the dc current is higher in the ac line voltage of the 120 V case by nearly 20 A. Having a greater ac line voltage allows the battery to be charged to a higher voltage and charges the battery at a higher current.

3.6 Battery

The battery provides excitation for the synchronous generators and powers the dc loads. During emergency loss of normal electrical power, the battery can provide power to the ac loads for a limited time through the inverter and transformer. Electrochemical modeling is not used for this battery model because it involves a system of coupled time-varying partial differential equations that are computationally expensive to solve [16]. Electrochemical modeling both describes various parameters such as mass, energy, and momentum transport and captures the kinetics and thermodynamics of the chemical and electrical electrochemical reactions. Electrochemical modeling includes both macroscopic and microscopic quantities that capture the mass transfer, charge-transfer reactions, current density, diffusivity, conductivity, the electrolyte and current flow through the polymer/salt phase [17].

Instead, an electrical circuit modeling approach that involves resistances and capacitances that represent time constants in Thevenin equivalent circuits [18] has been implemented. Only second, minute and hour time constants are considered. There are no partial differential equations in the electrical circuit modeling approach, which simplifies the simulation and shortens simulation time.

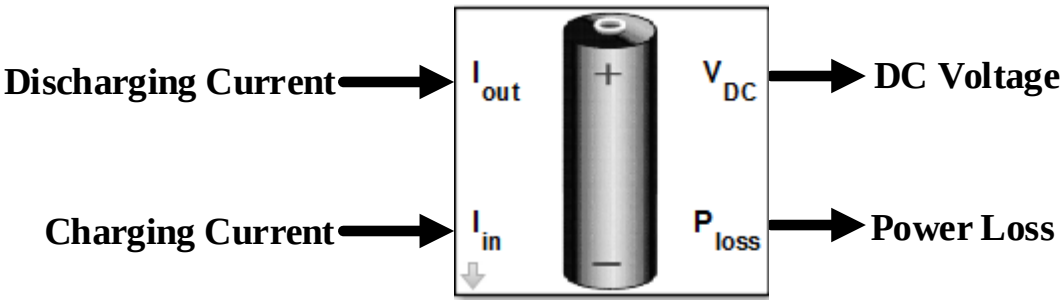

Figure 30: Battery model with inputs and outputs

The inputs to the battery module model shown in Figure 30 are

- I_{out} - Discharging dc current from the dc loads (A)
- I_{in} - Charging dc current from the transformer rectifier (A)

The outputs to the battery module model are

- V_{dc} - DC voltage from the battery sent to the dc buses or dc loads (V)
- P_{loss} - Power loss in the battery due to internal resistances (W)

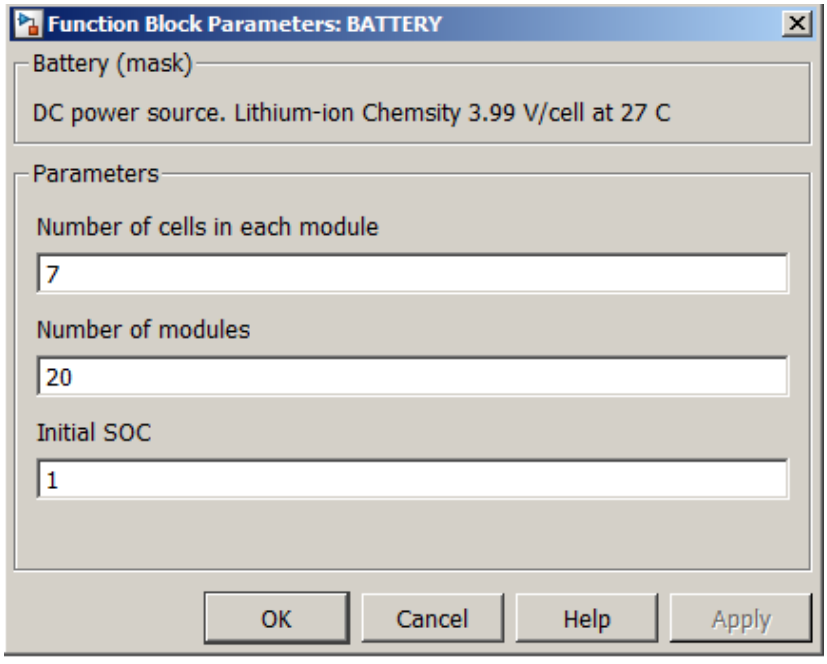

Figure 31: Battery property menu

In the battery property menu as seen in Figure 31, the following inputs can be put in:

- N_{cell} - Number of series cells in each string
- N_{mod} - Number of parallel strings to form a module
- $SOC_{initial}$ - Initial state of charge of the battery module

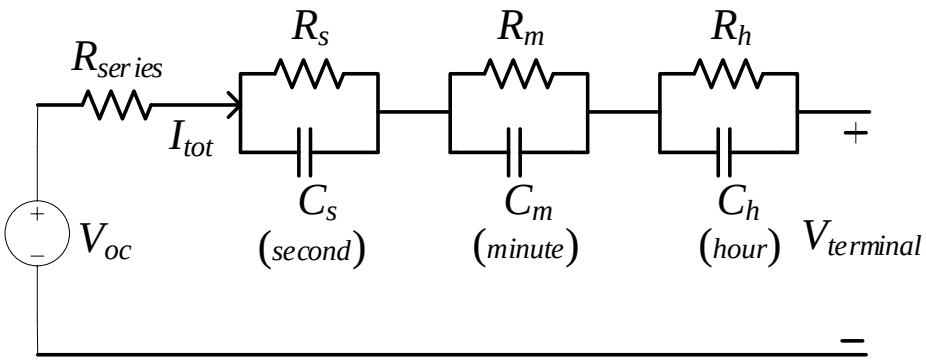

Figure 32: Battery cell circuit diagram

The electrical circuit modeling approach is based on the battery circuit diagram in Figure 32. In order to calculate the battery voltage, the steps proposed in literature [18] can be seen in Figure 33.

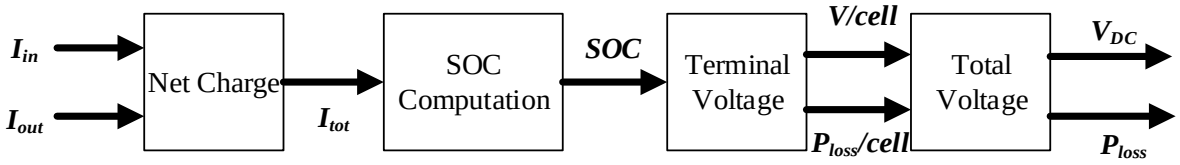

Figure 33: Battery model overview

Increasing the number of parallel modules increases the current capacity of the battery module. The total current through the circuit is

$$I_{tot} = N_{mod}(I_{out} - I_{in}) \tag{28}$$

The battery capacity is a function of the charging and discharging rates, temperature, cycle number, and a rate factor of the current. The rate factor accounts for undesired side reactions that increase with current discharge. The main attribute of the battery is the energy capacity or the

state-of-charge. For this model the parameters are represented as a polynomial function of SOC up to the sixth order with coefficients given by

$$SOC\left[i(t), T(t), n_{cycle}, t \right] = SOC_{initial} + \int f_1\left[i(t), T(t), n_{cycle}, f(i(t)), t \right] dt \qquad (29)$$

For each resistance and capacitance, a nonlinear function of SOC is used. For each parameter a polynomial function of SOC up to the sixth order is given where the polynomial expression is determined from experimental results. The various time constants are parallel combinations of resistances (R) and capacitances (C) which, as seen in the circuit diagram in Figure 32, are functions of the state of charge:

$$R(or\ C) = A_0 + A_1 \cdot SOC + A_2 \cdot SOC^2 ... \qquad (30)$$

Once the resistances and capacitances are calculated using (24), the terminal voltage per cell can be calculated as

$$V_{\text{terminal}} = V_{oc} - I_{tot}\left(R_{series} + \left(R_s \,||\, \frac{1}{sC_s} \right) + \left(R_m \,||\, \frac{1}{sC_m} \right) + \left(R_h \,||\, \frac{1}{sC_h} \right) \right) \qquad (31)$$

By using (25), the output dc voltage of the battery is

$$V_{dc} = N_{cell} \cdot V_{terminal} \qquad (32)$$

where a single-cell lithium-ion battery can provide 3.99 V at 27 ºC when $SOC_{initial}$ is 100%. While this battery model can be adapted to other chemistries, extensive testing is required to determine the state-of-charge equation parameters as well as the resistances and capacitances.

The battery model simulated has been set to 7 cells in each module and 50 modules and initial state of charge of 100%. The waveforms in Figure 34 are generated from the total current out of the battery or discharge rate. Negative values mean that the battery is being charged and positive values mean that the battery is discharging.

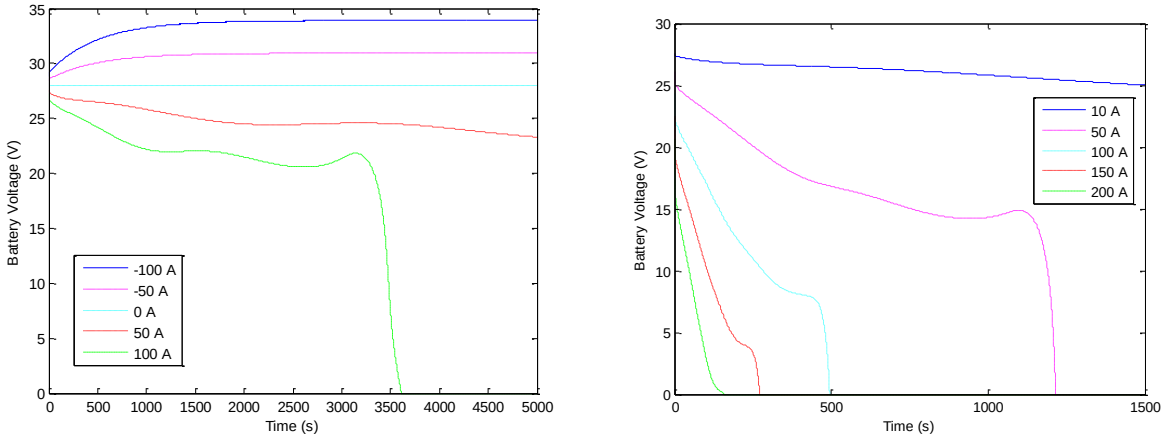

Figure 34: Battery voltage waveforms at different discharge rates

The voltage waveforms in Figure 34 roughly resemble the typical lithium-ion battery voltage waveform with a useable discharge range and then sharp voltage drop-off. For larger discharge rates the battery voltage will drop off much faster. These waveforms are not smooth with increasing voltages during the useable discharge range because of the polynomial expressions used to solve the resistances and capacitances of the time constants in (31). Additional time constants can be used to more accurately model or smooth out the voltage waveforms.

3.7 Electrical Loads

In recent decades, the power requirements for aircraft have increased significantly with the incorporation of more-electric designs such as electrically actuated landing gear, avionics, and anti-icing systems [9]. The electrical loads are divided into ac load and dc loads.

3.7.1 AC Loads

The majority of the power is used for the ac loads, which primarily consist of ac motors. The ac loads can be characterized as either constant power, constant current, or constant impedance. All three of these types of loads are accommodated by this model. The loads are assumed to be lumped and the voltages between them are the same. This assumption is used because line resistances and impedances are neglected. All of the work the ac load does becomes heat.

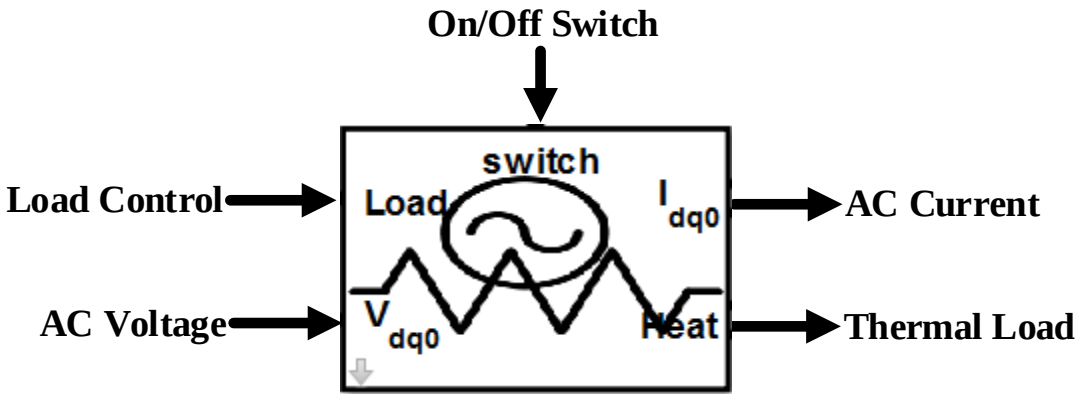

Figure 35: AC load model with inputs and outputs

The inputs to the ac load model seen in Figure 35 are

- Switch - Boolean input that turns the load on or off
- Load control - A vector that describes the ac load $\begin{bmatrix} P_{load} & Q_{load} & I_{load} \end{bmatrix}$
- $\boldsymbol{v}_{dq0}$ - Synchronous reference frame line voltage from the generator (V)

The outputs to the ac load model are

- $\boldsymbol{i}_{dq0}$ - Synchronous reference frame line current sent to the generator (A)
- ***Heat*** - Thermal load (W)

The ac load model can be defined as either constant power, constant current, or constant impedance for different requirements. The load control is how each of these types of ac loads is defined. The load control is a vector that defines the ac load's real power, reactive power, and current and can be used to define the constant power and constant current loads. Constant impedance loads can be defined in the ac load model property menu shown in Figure 36.

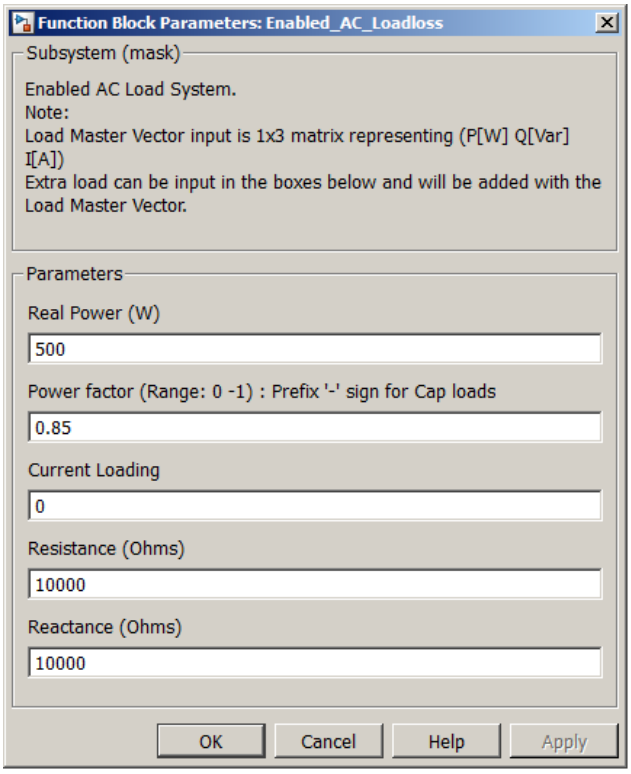

Figure 36: AC load property menu

In the AC load property menu shown in Figure 36, the following parameters can be defined:

- $\boldsymbol{P_{load}}$ - Real power (W)
- $\boldsymbol{PF}$ - Power factor
- $\boldsymbol{I_{load}}$ - Current load (A)
- $\boldsymbol{R}$ - Resistance (Ω)
- $\boldsymbol{X}$ - Reactance (Ω)

The ac loads defined in the property menu remain constant throughout the simulation. For characterizing ac loads that vary over time, the load control input must be used. One example of how to use the load control input is to define the varying variables in a one-dimensional lookup table. The output of each would be a gain that defines if the load is real power, reactive power, or current as shown in Figure 37.

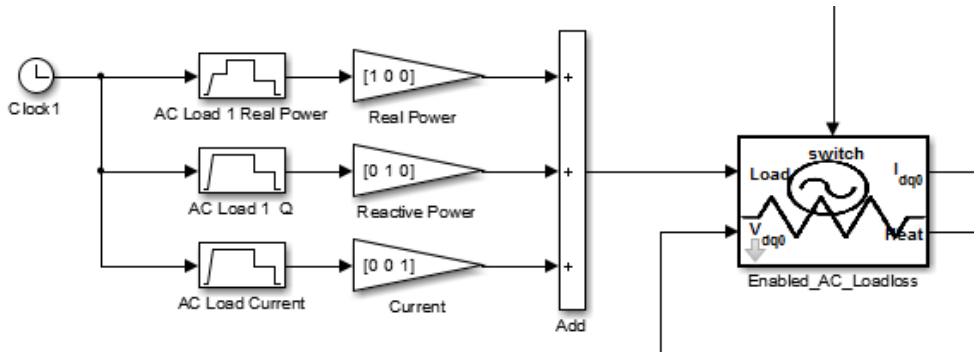

Figure 37: Defining ac loads with load control

For given values of real and reactive power, P and Q, the direct and quadrature, I_d and I_q, currents are

$$I_d = \frac{P_{load}V_d + Q_{load}V_q}{V_d^2 + V_q^2} \text{ and } I_q = \frac{P_{load}V_q - Q_{load}V_d}{V_d^2 + V_q^2} \tag{33}$$

Additionally, for constant impedance loads, the direct and quadrature currents are

$$I_d = \frac{RV_q + XV_d}{R^2 + X^2} \text{ and } I_q = \frac{RV_q - XV_d}{R^2 + X^2} \tag{34}$$

The output synchronous frame line current is the sum of Equations (27) and (28) in their respective axes. The electrical loads eventually become heat that is routed to the thermal system for thermal management.

3.7.2 DC Loads

The dc loads come from avionics and lighting. The dc loads are defined as constant power or constant current loads. Like the ac loads, the dc loads are lumped together where their voltages are assumed to be the same. All of the work the dc loads becomes heat. For a MEA architecture, the dc loads will increase as seen in the use of dc motors for the Boeing 787 [23].

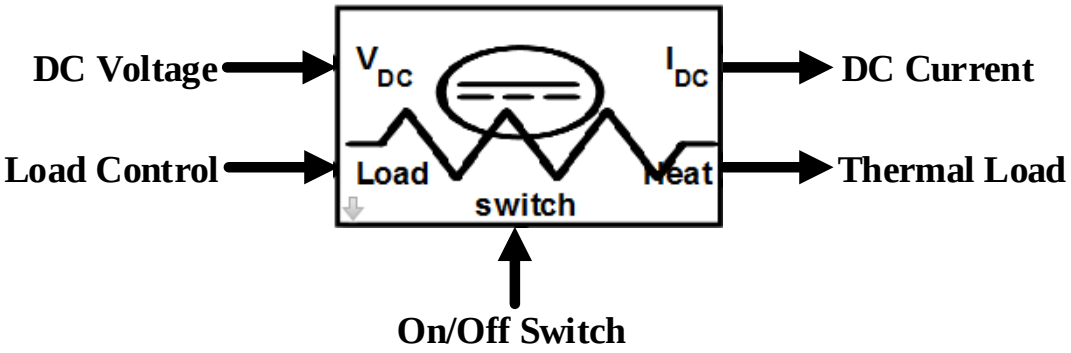

Figure 38: DC load model with inputs and outputs

Similar the ac electrical loads, the inputs to the dc load model seen in Figure 38 are

- Switch - Boolean input that turns the load on or off
- $\boldsymbol{V_{dc}}$ - DC voltage from the battery (V)
- Load control - A vector that describes the dc loads $\begin{bmatrix} I_{load} & P_{load} \end{bmatrix}$

While the output to the dc load is

- $\boldsymbol{I_{dc}}$ - DC current sent to the battery (A)
- ***Heat*** - Thermal load (W)

The first element of the load control vector consists of the constant current loads, while the second element consists of the constant power loads. Figure 39 illustrates an implementation of the load control vector into the dc load model.

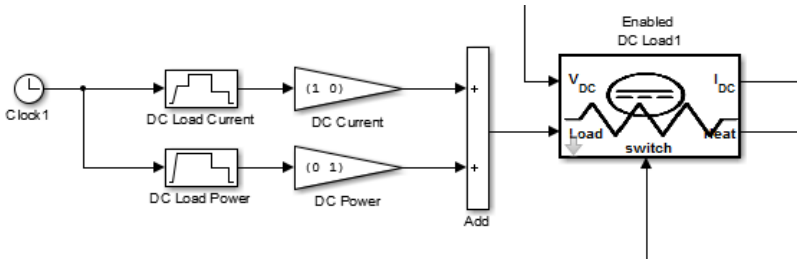

Figure 39: Defining dc loads with load control

For the dc load, the output dc current is defined as

$$i_{dc} = \frac{P_{load}}{V_{dc}} + I_{load} \tag{35}$$

4 SIMULATION RESULTS

The previous chapters described the various component models that have been built for an aircraft electrical system. The component models can be assembled together to form a complete electrical system for a civil aircraft. Since each component is modular and scalable, different aircraft architectures are supported for modeling and simulation. For a complete model and simulation, a Numerical Propulsion System Simulation (NPSS) engine model has been used to simulate the engine with a sample flight profile. NPSS is a multi-physics simulation environment initially developed by the National Aeronautics and Space Administration to model complete aircraft engines [24]. It is currently managed by the NPSS Consortium of Southwest Research Institute who update the capabilities, interfaces, and models [25]. The engine model, which was developed in the NPSS environment, for a Boeing 737 was provided by Rolls-Royce.

4.1 Flight Profile and Engine

An aircraft's flight profile is a breakdown of the flight functions during different stages. For different flight profiles and stages, the performance and operation of the aircraft change. The stages of the flight profile include taxiing, take-off, climb, cruise, descent, approach, and landing. The parameters used to define the stages of the flight profile are altitude, mach number, and thrust.

The sample flight profile used to simulate the aircraft electrical system is roughly 5.3 hours and incorporates the following phases:

1. Start-up — Docked at airport gate
2. Taxi out — From gate to runway
3. Take-off — From runway to the air
4. Climb — Increasing altitude

5. Cruise Leveled flight
6. Descent Lowering altitude
7. Loiter Leveled flight at lower altitude
8. Approach Lowering altitude before landing
9. Landing During landing
10. Taxi on from runway to destination gate

The graphical representation of the sample flight profile in Figure 40 shows the changes in the altitude and thrust that are inputs to the engine model. Mach number is also needed for the engine model shown in Figure 41.

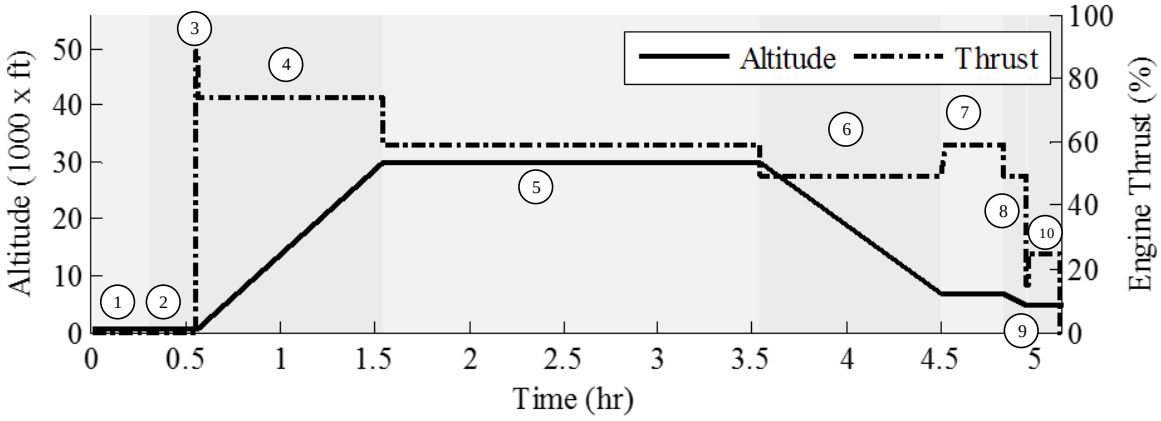

Figure 40: Sample flight profile

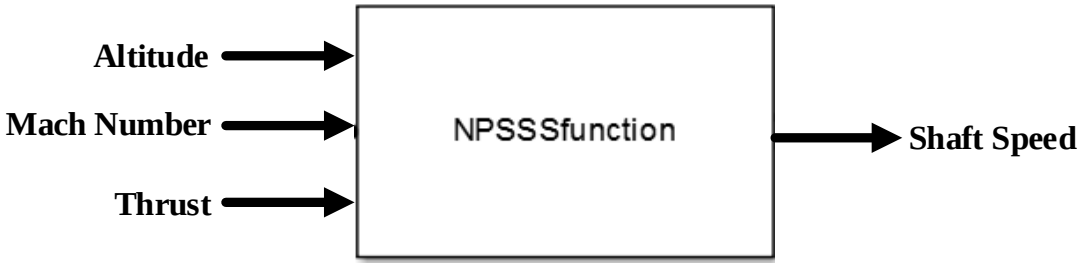

Figure 41: Simulink NPSS engine model

The outputs to the engine model include net thrust, bleed air temperature, bleed air pressure, fuel flow, and spool speeds. The only output used by the electrical sub-system is the engine shaft

speed from the spools used by the generators. The engine model is controlled by an S-function that checks for certain input variables. By testing various inputs, the engine model contains a numerical solver with a maximum number of iterations until convergence set to 1000 as opposed to look-up tables. The numerical model makes use of a Jacobian matrix and therefore can generate errors if the matrix is singular. The setup for the engine model is shown in Figure 55 in Appendix A.

4.2 Boeing 737 Architecture

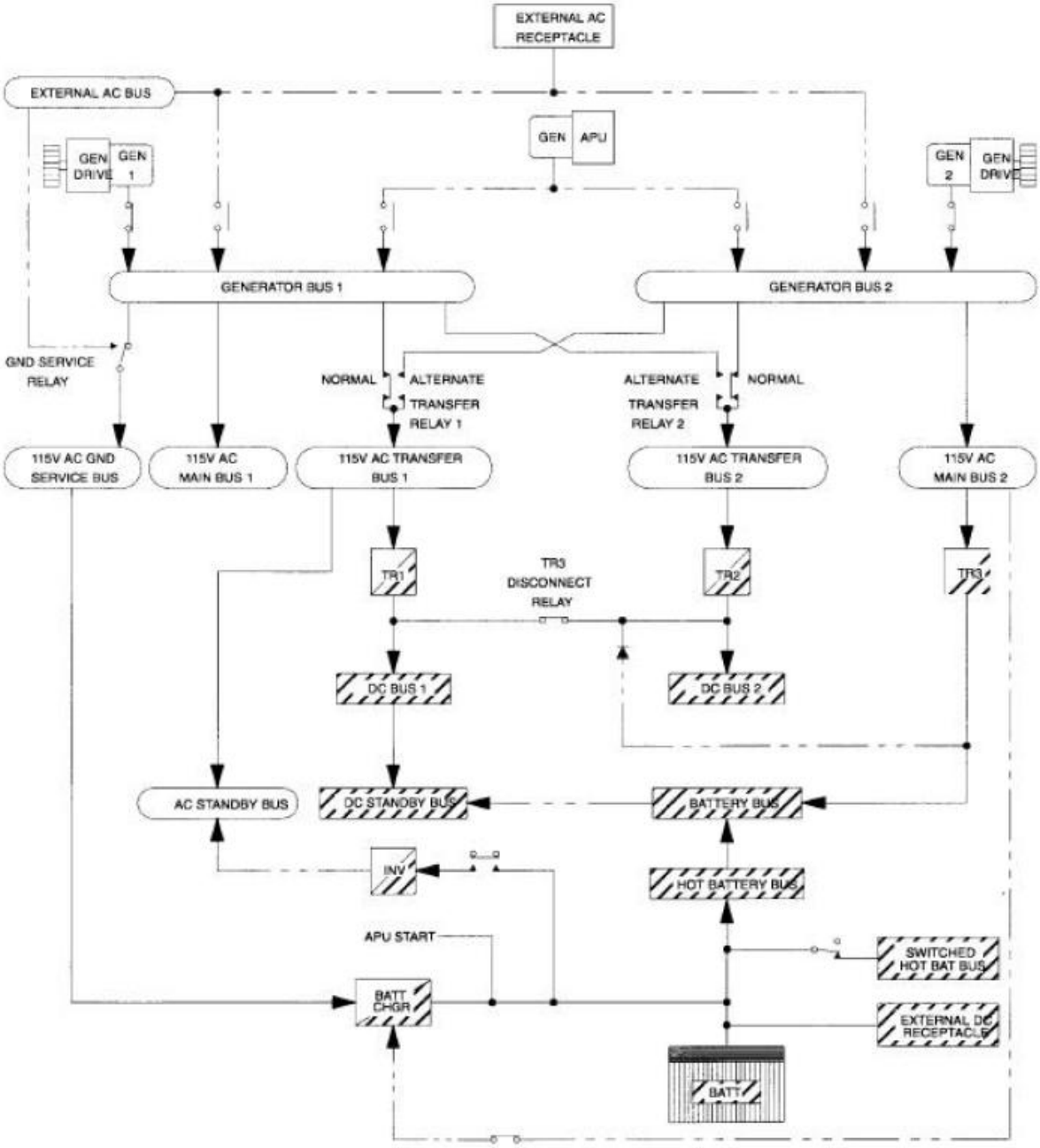

Figure 42: Boeing 737 Electrical Schematic taken from [10]

For the simulations, the Boeing 737 aircraft was chosen to be modeled because it is a typical twin-engine aircraft frequently used in commercial air travel. The electrical schematic of the Boeing 737 is shown in Figure 42 from [10]. Besides the electrical schematic [10], the

operation of each component is described. The power sources of the Boeing 737 include two synchronous generators, a secondary generator system called the auxiliary power unit (APU), and a battery. The twin-engine Boeing 737 is capable of supporting 180 kVA [9] (90 kVA from each generator). The APU is composed of a synchronous generator driven by a gas turbine engine.

There are various power distribution buses that route and reroute power through the electrical system for safe operation. The main power distributions seen in Figure 42 are the generator, main, transfer, and dc buses. Each of the two main generators is connected to its own generator bus, while the APU is connected to both generator buses in the case of either generator or engine failure. The generator buses are connected to the main buses that are attached to the ac loads. The generator buses are also connected to the transfer buses that are connected to the transformer rectifier units and then to the dc buses. The dc buses are connected to the battery and to the dc loads.

The basic schematic for a MEA will be similar to the Boeing 737 schematic, where the power sources are connected to the power distribution buses and then to the electrical loads and power converters. The additional electrical loads of a MEA will require either bigger generators or more generators. Increasing the number of generators is preferable as it also increases the reliability of the power generation. The Boeing 787 has six generators, two per engine, and two APU generators [23].

4.3 Basic Simulink Simulation

The Boeing 737 aircraft architecture was modeled using the components and the schematic described previously. Throughout the model, Simulink "Goto" and "From" tags are used to simplify the model and improve the organization. These tags convert the signal wires between

components to a wireless signal between the "Goto" and "From" tag. Without these tags, signal lines would be run throughout the Simulink model. The tags are also color coded to indicate what kind of connection they are. Red is used for dc voltage. Blue is used for ac current. Purple is used for dc loads. Orange is used for ac loads. White is used for dc current. Green is used for thermal loads that will be sent to the thermal sub-system for thermal management. Yellow is used for the rest of the miscellaneous connections.

In this simulation of the Boeing 737, the generators and APU were sized to 100 kVA with the nominal voltage set to 115 VAC. Under normal operation for the Boeing 737 the ac voltage is 115±5 VAC and the dc voltage is 26±4 VDC [11]. Since the battery voltage is rated for 26 V, the number of parallel cells of the battery model is set to 7 cells per module to provide 28 V. The number of modules is set to 50 modules for a capacity of 110 A-h so the battery can last throughout the duration of the flight profile.

The modularity of this toolset allows individual components to be added, removed, or exchanged with ease. However, all of the component interfaces must be connected in a specific way to another component. As mentioned previously and shown in Figure 2 and Figure 42, the power sources are connected to buses where they impose a voltage signal on the bus and receive a current signal. The buses are connected to the electrical loads or power converters where they impose a voltage signal on both electrical loads and power converters and receive a current signal. Sometimes a component will receive multiple signals of the same type from different components. For example, the auxiliary battery receives multiple dc current signals from each of the generator outputs. A summation block is used before the component to combine those signals into one input signal. The model is complex and broken up into two sections, ac and dc. The complete overview of the electrical system model can be seen in Figure 56 in Appendix A.

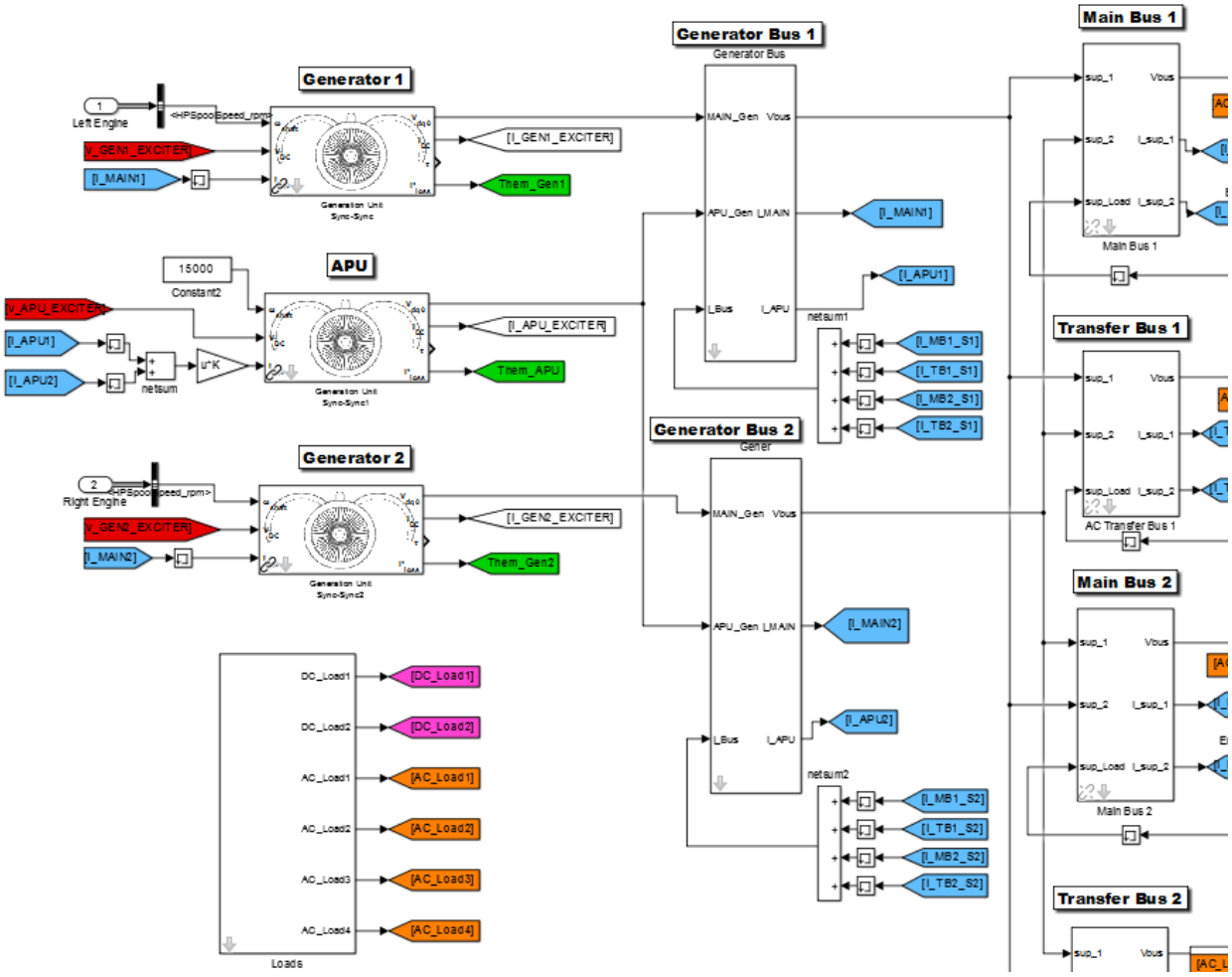

Figure 43: Boeing 737 model including generators, ac buses, and load

Figure 43 illustrates the left side of the Boeing 737 model. The generators are placed in the far left with the inputs described in Section 3.1. The generator output ac voltage is imposed on various buses that direct the ac voltages to the appropriate electrical load and the currents to the appropriate generator. In the left corner is the loads block where the various electrical loads are defined and consolidated. The output to this block is the load control signal that goes to the ac and dc loads.

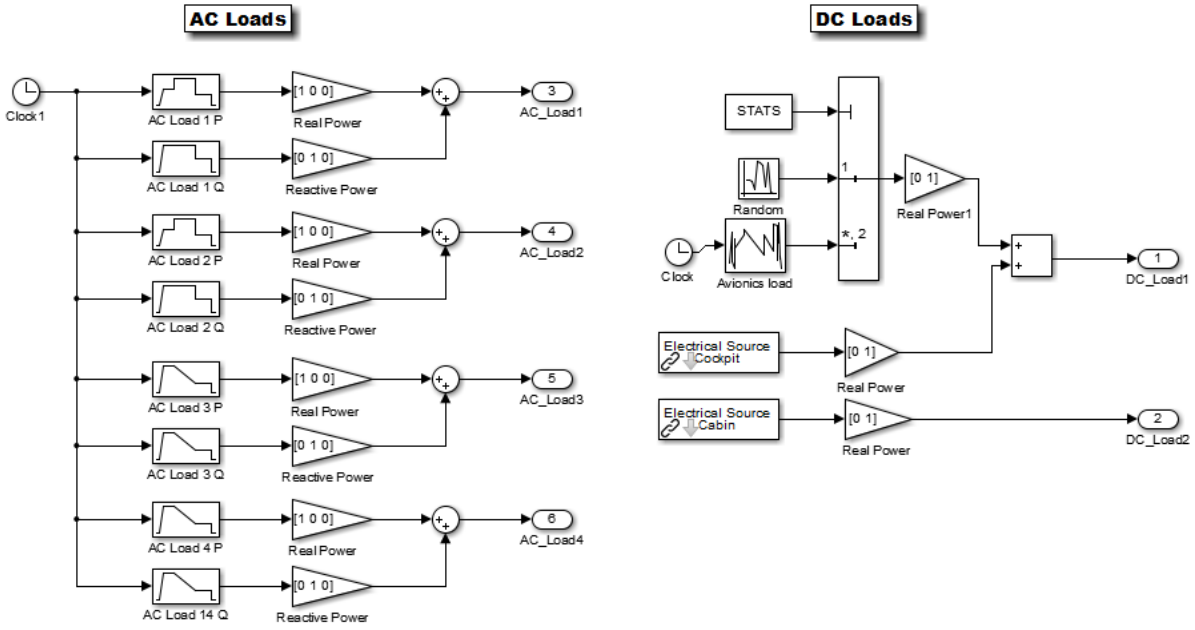

Figure 44: Load block defining ac and dc loads

Figure 44 illustrates the inside of the load block. Simulink "Lookup" tables are used to define the dynamic nature of all the electrical loads. Simulink "Gain" blocks are used to put load information for the "Lookup" tables into proper form as the load control vectors that go into the ac and dc loads. The sample electrical load profiles shown in Figure 45 were used. The ac load profile changes for the different phases of the flight profile. The ac load profile can be customized for different flight profiles.

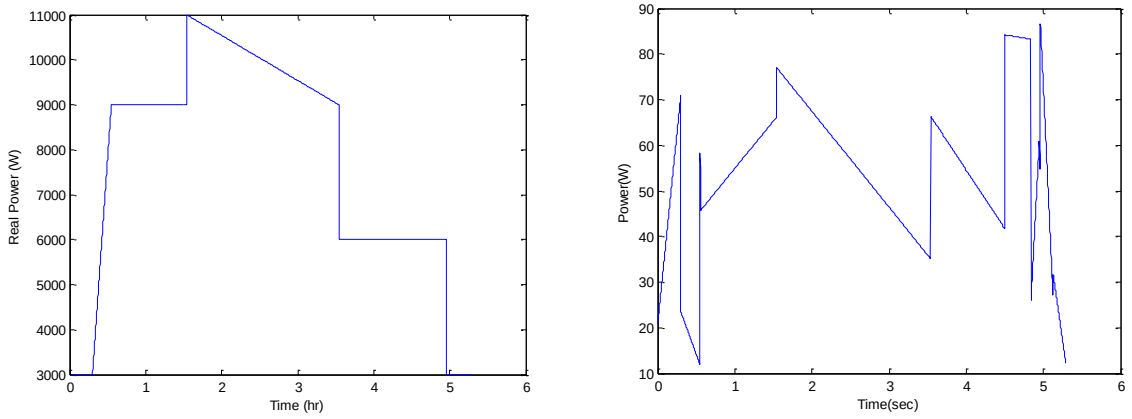

Figure 45: Real ac power and dc power demand waveform

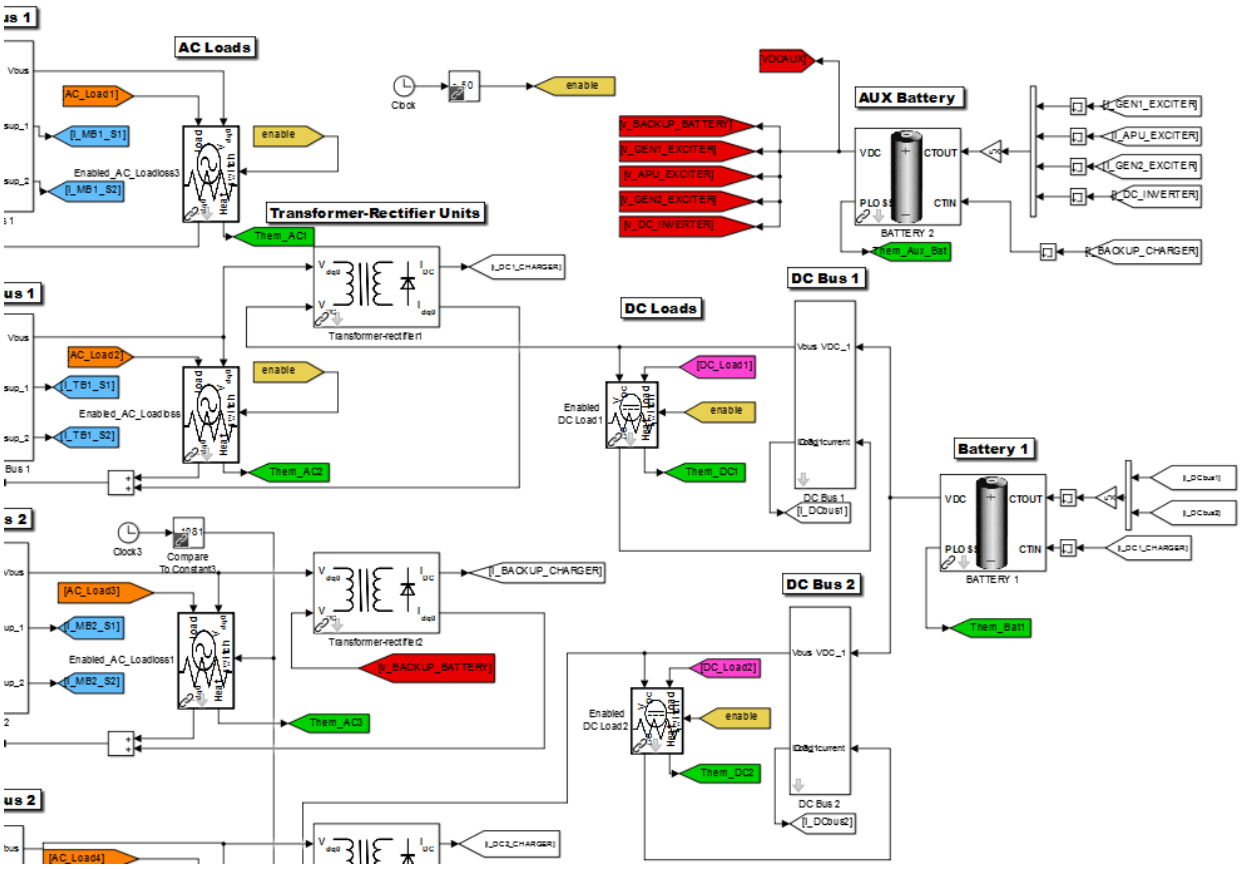

Figure 46: Boeing 737 model including batteries, dc buses, loads and TRU

The other half of the Boeing 737 model is shown in Figure 46. The main and transfer buses are each connected to an ac load. An arbitrary 50 s delay is set using the on/off switch of the electrical loads. This gives time for the generators to build up voltage before being loaded. The ac voltage is imposed on the loads and an ac current signal is sent back to the buses and ultimately back to the generators. All the main and transfer buses except main bus 1 are connected to a transformer rectifier unit. The TRUs are used to recharge the batteries. The batteries are on the far right side. The main battery is connected to the dc buses while the auxiliary battery is connected to the generators. The auxiliary battery is only used to provide excitation for the generators so the tags are to and from all of the generators. One of the TRUs charges the auxiliary battery. The main battery imposes its dc voltage on both of the dc buses.

The dc buses impose that dc voltage signal on the dc loads and the TRU. Both of those components send a dc current signal back. The dc load current is discharging current for the battery and the TRU is charging current for the battery. They go into different inputs for the battery described earlier in Section 3.5.

As mentioned previously, the toolset and this sample electrical system model are designed to interface with other aircraft systems. The engine shaft is linked to the generator shaft via a gearbox that reduces the generator shaft speed. The generator feeds back a torque that affects the performance of the engine. All of the electrical losses generated from the various components are converted into heat or thermal loads that are routed to the thermal system.

While a basic setup for a sample Boeing 737 architecture was just described, the same process can be used to set up different aircraft architectures. Generator block models can be easily added or removed. If a generator block model is added, it must be connected to a battery and a generator bus block must be added. Another battery model can be added such that each dc bus is powered by one battery model. The transformer rectifier units can be removed to see if the battery can supply all of the dc loads for an entire flight. Ultimately the user can use the toolset to build or customize any aircraft architecture.

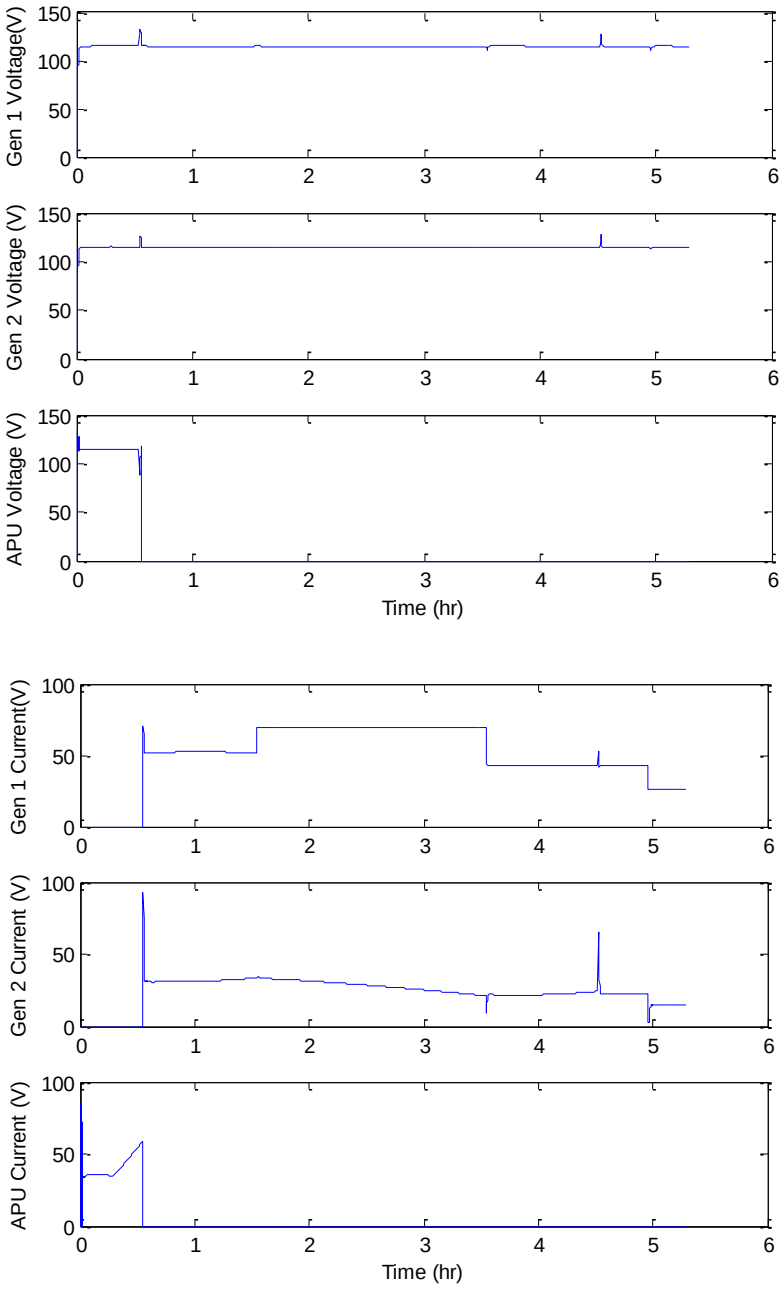

Figure 47: Generator voltage and current outputs during simulation

The first sample simulation uses the basic setup for Boeing 737 described. The resulting generator and APU voltage and current waveforms of Figure 47 show a stable simulation of the 5.3 hr flight. All of the generator voltages are brought up and maintained at 115 V. The APU supplies power for taxi and then the generators supply power for take-off and the rest of the

flight. There are voltage and current spikes that appear at the 0.5 hr mark and 4.5 hr mark, which correspond to take-off and to the transition from descent to approach. Both of these events are associated with an increase in thrust that increases the engine shaft speed and therefore generator speed. The increase in shaft speed increases the voltage as shown previously in Figure 13. These voltage spikes can be reduced by changing the parameters of the voltage regulator of the generators or by increasing the size of the generator.

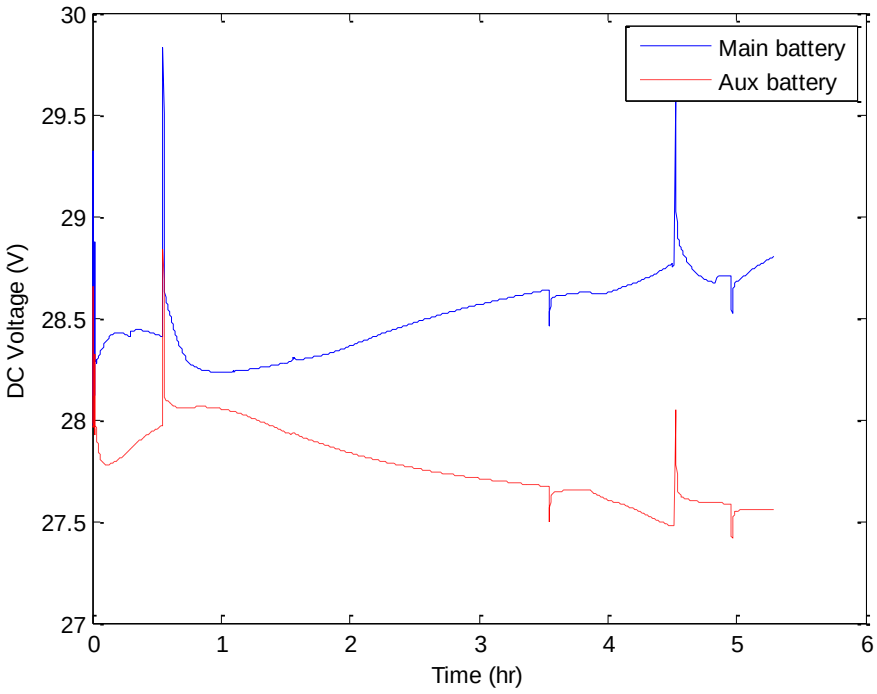

Figure 48: Battery voltage during simulation

During the first simulation, the battery voltages are stable and maintained in the rated 26±4 VDC range as shown in Figure 48. Both battery voltages are changing because they are being simultaneously charged by the generators while discharging to supply power to the dc loads or excite the generators. The spikes in voltage occur at the same time as voltage and current spikes in the generators.

The various power flows throughout the electrical system are ac power, dc power, and heat. All of the ac power and dc power goes to the electrical loads and becomes heat. All of the heat is gathered in a summation block and sent to the thermal sub-system for thermal management. These signals do not have to be summed and can be sent separately to account for their distinct locations within the aircraft. For example, some of the heat is passively released through the airframe to the environment and some of the heat is actively dealt with by the aircraft heat exchangers.

4.4 Single Generator Temporary Failure

Even though aircraft are built to be reliable with redundant systems, different faults and failures happen during flight. Sometimes the failure is temporary and normal operation can be resumed. A temporary disconnection and then reconnection between a generator and its generator bus has been adapted from the previous simulation to illustrate the simulator capability. The generator and battery properties remain the same. The ac and dc load information has not been changed. "Switch" blocks with attached "Clock" blocks were used to instantly cut the generator component inputs and outputs from the other blocks at the time of fault. Figure 49 illustrates the voltage and current waveforms associated with such an event.

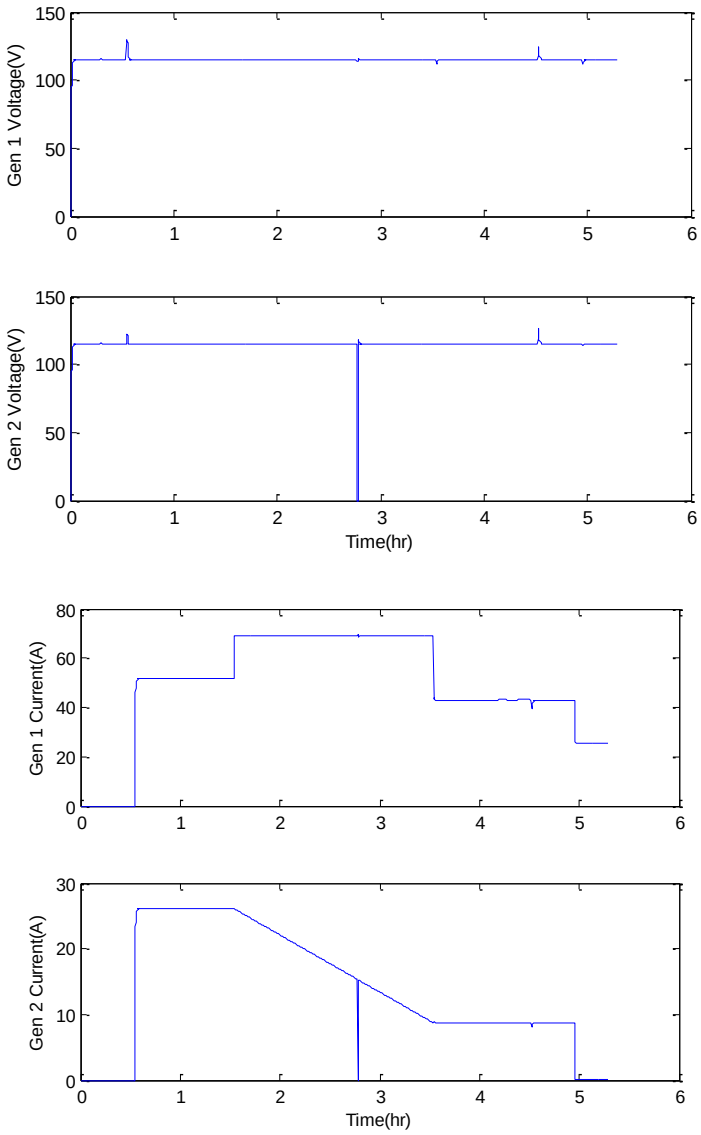

Figure 49: Generator voltage and current waveform for temporary power voltage

For this simulation, at the 2.78 hr (10000 s) mark, there is a disconnection between generator 2 and its generator bus. Generator 2 is still operational but not electrically connected to its bus and loads. The voltage and current coming from generator 2 drop to zero. This failure lasts for 30 seconds, and then generator 2 is reconnected. When the generator and generator bus are reconnected there is a spike in voltage and some overshoot as the control system brings its

voltage back to the nominal value of 115 V. The Boeing 737 model can handle temporary disconnections to one of the main power sources and no corrective action is required.

4.5 Single Generator Complete Failure

Compared to the previous simulation, in some cases the generator will fail and will be down for the duration of flight. In those cases, the various redundancies of the aircraft are used and corrective action is required. The loss of an engine or generator is a major event that involves many steps. First, some of the noncrucial electrical loads like in-flight entertainment are shed as specified by the user. Then, the APU is started up by the pilot to replace the lost generator and some of the load is taken on by the other remaining generator. The shaft speed of that generator is increased to account for that. As mentioned in the previous section, "Switch" blocks with "Clock" blocks were used to simulate the generator failure. The electrical loads are actively reduced after the failure happens. Figure 50 illustrates the voltage and current waveforms of the generators and APU during a generator failure.

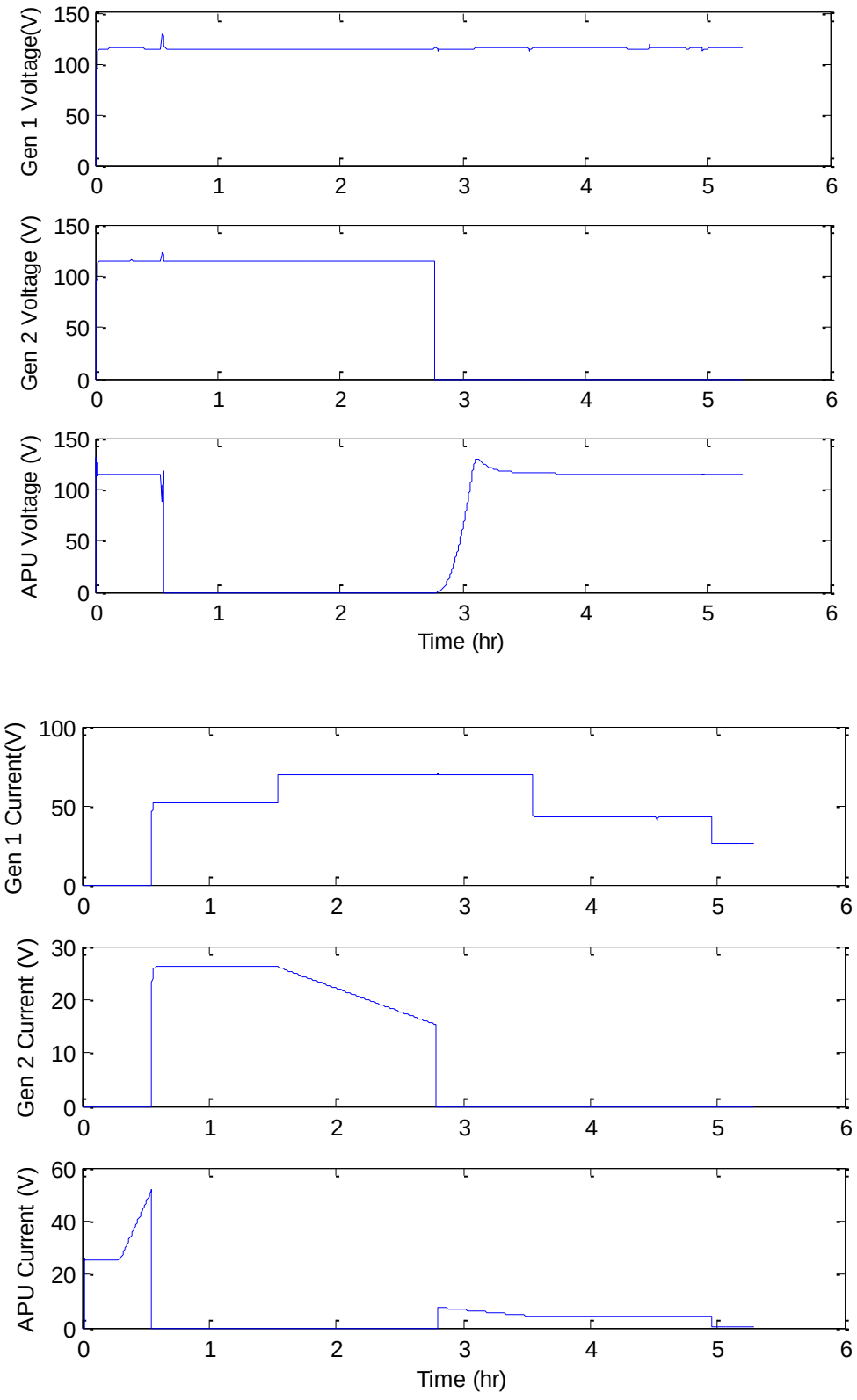

Figure 50: Voltage and current waveforms during generator 2 failure

This final simulation is modified from the temporary fault case where corrective action of load shredding and starting up the APU is necessary. The generators and APU are powered for taxi. During taxi, the APU provides the power for all the electrical loads. For take-off, the APU is powered down, and the two generators are used. At the 2.78 hr mark, generator 2 fails, and shortly thereafter the thrust in generator 1 increases to account for the added load it will have to power. Compared to Figure 49, the voltage in generator 1 increases due to the shaft speed increase. Also, the APU is powered up and the some of the electrical loads to generator 2 have been reduced. The APU then replaces generator 2 for the rest of the flight.

While other individual component failures can be modeled such as the TRU or the battery, there are some failures that cannot be modeled using this toolset. This toolset cannot model single-phase failures of the generators. Since none of the components are modeled as temperature dependent, overheating of components cannot be modeled. For this sample Boeing 737 configuration, if both generator buses fail, there is no power flowing to any of the ac loads. Similarly if both of the dc buses fail, there is no power flowing to any of the dc loads. The other failures that cannot be modeled using this standalone electrical toolset are those associated with the other aircraft sub-systems.

5 CONCLUSIONS

A toolset composed of various component models has been created to model and simulate the power flow of the electrical system of various aircraft architectures over an entire flight. The toolset has been created using the MATLAB/Simulink environment. The component models were designed to be modular and scalable, so each component can be replaced and different aircraft architectures can be modeled and simulated. The components were designed to be intuitive with property menus and help files so the user can build the model. Each of the components for building an aircraft electrical system have been described with the engineering and mathematical approach. In order to support fast simulations to integrate with other aircraft systems, many of the components were simplified using ideal or averaged models.

A sample electrical system of a Boeing 737 was modeled and simulated with appropriately scaled components to show the stable simulation of a 5.3 hr flight and some of the capabilities of the toolset. The electrical system included power sources, power converters, power buses, and electrical loads. Besides normal operation, the toolset can be used to model and simulate faults and failures that may require corrective actions. For the fault simulation of a temporary disconnection between a generator and its generator bus, the connection was able to be restored with no corrective action necessary. For the final simulation of a single generator failure, corrective action of load shredding and using the APU generator was shown. With the focuses of scalability and modularity, the user can create any aircraft architecture and analyze different scenarios.

The development of this toolset is an ongoing process to make it accurate, fast, and easy to use. The scalability of the components can be improved. Some examples of improved scalability would be adding more generator preset values and adding in the different chemistries

for the battery model, which would require extensive testing as mentioned previously. Additional dynamic models for each component can be added to the toolset. These models can be more detailed, requiring more information from the user. One example is adding in temperature-dependent relationships to the electrical components. Finally as part of a collaborative project, the integration of this toolset will the other systems to understand their interactions is ongoing.

WORKS CITED

[1] I. Moir and A. Seabridge, *Design and Development of Aircraft Systems*, Chichester, West Sussex, United Kingdom: John Wiley & Sons, 2013.

[2] P. Krus, "Systems Engineering in Aircraft System Design," in *INCOSE International Symposium*, Melbourne, Australia, 2001.

[3] S. Bozhko, T. Wu, Y. Tao and A. G.M., "More-Electric Aircraft Electrical Power System Accelerated Functional Modeling," in *International Power Electronics and Motion Control Conference*, Ohrid, Republc of Macedonia, 2010.

[4] T. Wu, S. Bozhko, G. Asher and T. D.W.P, "Accelerated Functional Modeling of Aircraft Electrical Power Systems including Fault Scenarios," in *Industrial Electronics*, Porto, Portugal, 2009.

[5] R. Abdel-Fadil, A. Eid and M. Abdel-Salam, "Electrical Distribution Power Systems of Modern Civil Aircrafts," in *International Conference of Energy Systems and Technologies*, Cairo, Egypt, 2013.

[6] M. Yasar, H. Kwatny and G. Bajpai, "An Integrated Modeling, Simulation and Analysis Environment for Coupled Aircraft Subsystems to Facilitate Control Synthesis and Validation," in *AIAA Modeling and Simulation Technologies Conference*, Kizzimmee, Florida, 2015.

[7] S. L. Hanke, "A Model-Based Methodology for Integrated Preliminary Sizing and Analysis of Aircraft Power System Architectures," Doctoral Dissertation, Université de Toulouse, 2008.

[8] M. Williams, S. Sridharan, S. Banerjee and C. Mak, "PowerFlow: A Toolbox for Modeling and Simulation of Aircraft Systems," in *SAE AeroTech Congress & Exhibition*, Seattle, Washington, 2015 [submitted].

[9] I. Moir and A. Seabridge, *Aircraft Systems: Mechanical, Electrical, and Avionics Subsystems Integration*, Chichester, West Sussex, England: John Wiley & Sons, 2008.

[10] "SmartCockpit," [Online]. Available: http://www.smartcockpit.com/. [Accessed 25 Jan. 2015].

[11] Boeing, "Red Sky Ventures," 20 Nov. 1997. [Online]. Available: http://www.redskyventures.org/doc/other-poh/Boeing_737-600-700-800-900_Operations_Manual.pdf. [Accessed 15 Mar. 2015].

[12] R. Langton, C. Clark, M. Hewitt and L. Richards, *Aircraft Fuel Systems*, Chichester, West Sussex: John Wiley & Sons, 2009.

[13] P. W. Sauer, "Time-Scale Features and Their Applications in Electric Power System Dynamic Modeling and Analysis," in *American Control Conference*, San Francisco, CA, 2011.

[14] P. W. Sauer and M. A. Pai, *Power System Dynamics and Stability*, Prentice Hall, 1998.

[15] P. Krause, O. Wasynczuk, S. Sudhoff and S. Pekarek, *Analysis of Electric Machinery and Drive Systems*, Hoboken, New Jersey: John Wiley & Sons, 2013.

[16] D. W. Dees, V. S. Battaglia and A. Belanger, "Electrochemical Modeling of Lithium Polymer Batteries," *Journal of Power Sources*, pp. 310-320, 2002.

[17] M. Doyle, T. F. Fuller and J. Newman, "Modeling of Galvanostatic Charge and Discharge of the Lithium/Polymer/Insertion Cell," *J. Electrochem. Soc.*, vol. 140, no. 6, pp. 1526-1533, 1993.

[18] R. C. Kroeze and P. T. Krein, "Electrical Battery Model for Use in Dynamic Electric Vehicle Simulations," in *IEEE Power Electronics Specialists Conference*, Rhodes, Greece, 15-19 June 2008.

[19] S. Kharitonov, P. Bachurin, A. Geist, D. Makarov, M. Balagurov and D. Shtein, "Comparison of Dual Z-Source Inverter and Traditional PWM Inverters for Aircraft Power Generation System," *Actual Problems of Electronics Instrument Engineering*, pp. 108-113, 2-4 Oct 2012.

[20] P. Krein, *Elements of Power Electronics*, New York: Oxford University Press, 1997.

[21] A. M. Bazzi, P. T. Krein, J. W. Kimball and K. Kepley, "IGBT and Diode Loss Estimation Under Hysteresis Switching," *IEEE Trans. Power Electronics*, vol. 27, no. 3, pp. 1044-1048, Mar. 2012.

[22] "Machine Parameterization," The MathWorks, [Online]. Available: http://www.mathworks.com/help/physmod/sps/ug/machine-parameterization.html. [Accessed 30 May 2015].

[23] J. Hale, "Boeing 787 from the Ground Up," *AERO,* p. 21, Sept. 2006.

[24] J. K. Lytle, "The Numerical Propulsion System Simulation: An Overview," *NASA/TM-2000-209915* (National Aeronautics and Space Administration, Glenn Research Center, Cleveland, OH, 2000).

[25] D. Ransom, "Numerical Propulsion System Simulation (NPSS®) Consortium," Southwest Research Institute, [Online]. Available: http://www.swri.org/npss/. [Accessed 20 May 2015].

APPENDIX A: SIMULINK MODELS

This section includes the diagrams of the Simulink models

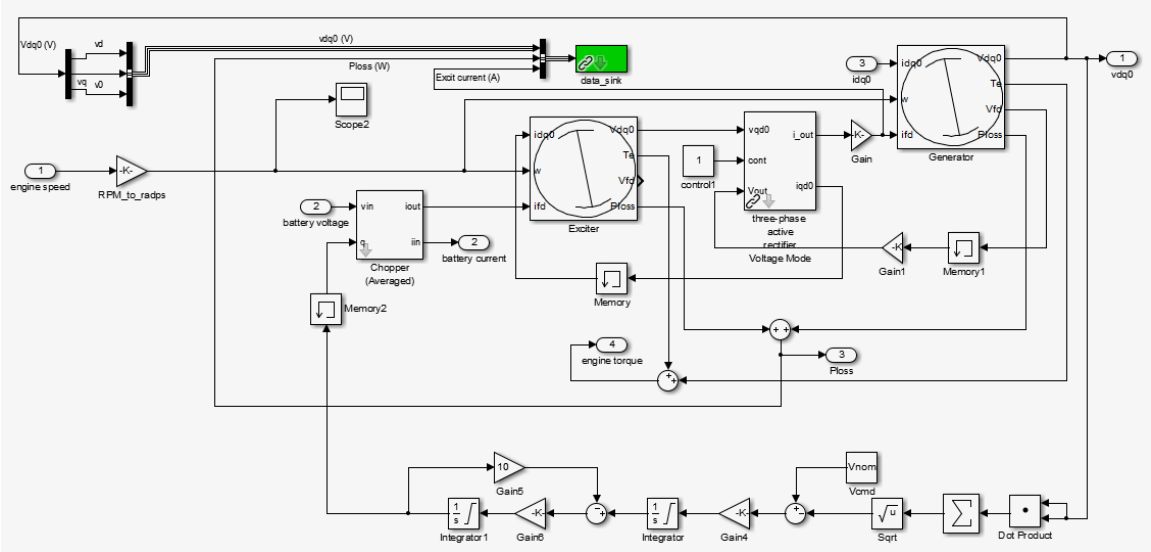

Figure 51: Simulink generator model

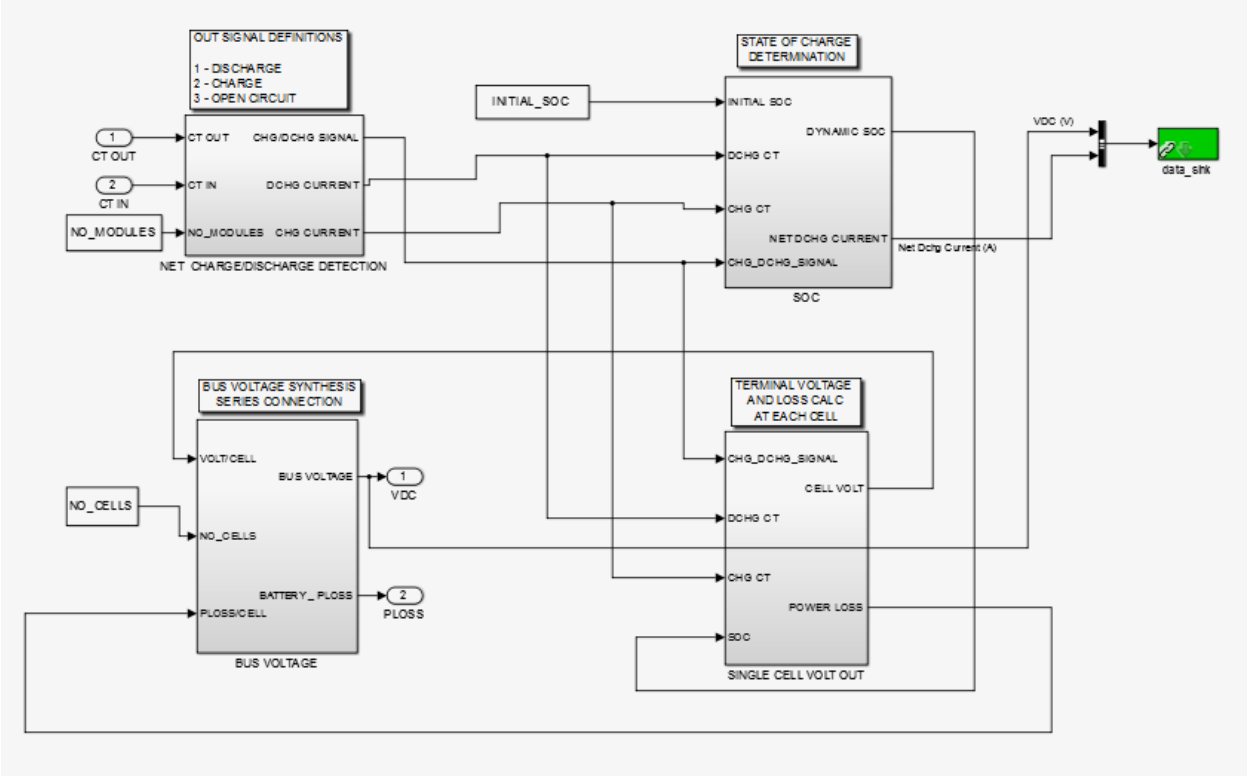

Figure 52: Simulink battery model

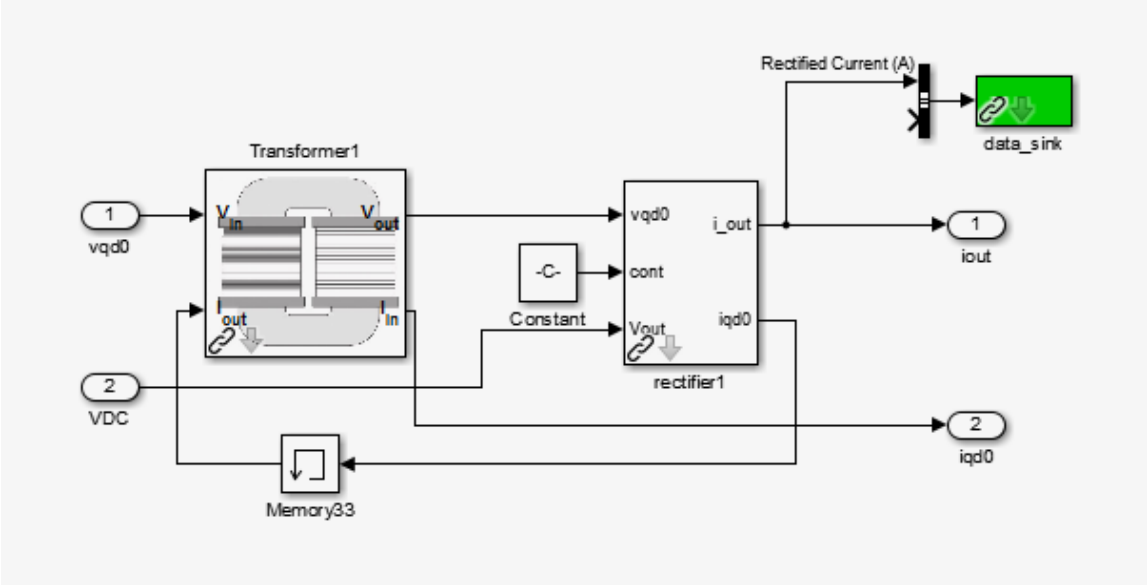

Figure 53: Simulink TRU model

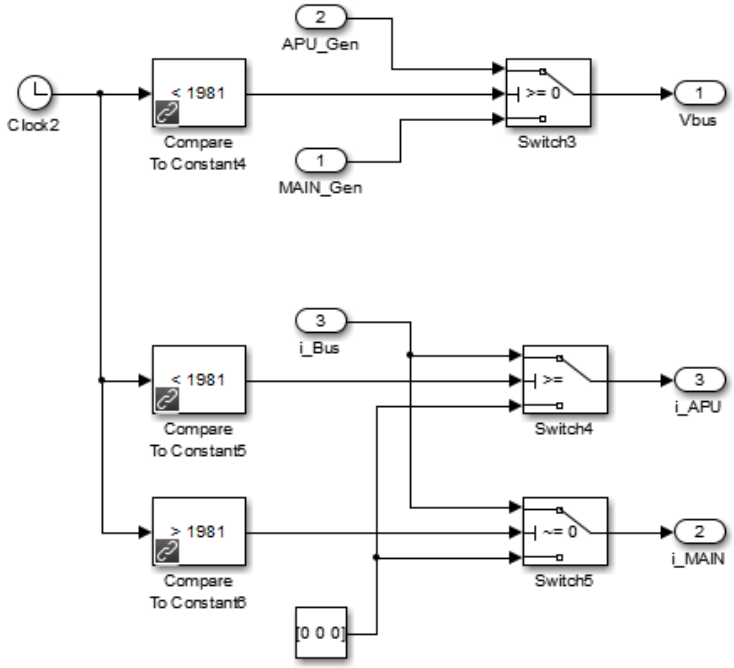

Figure 54: Simulink sample bus structure

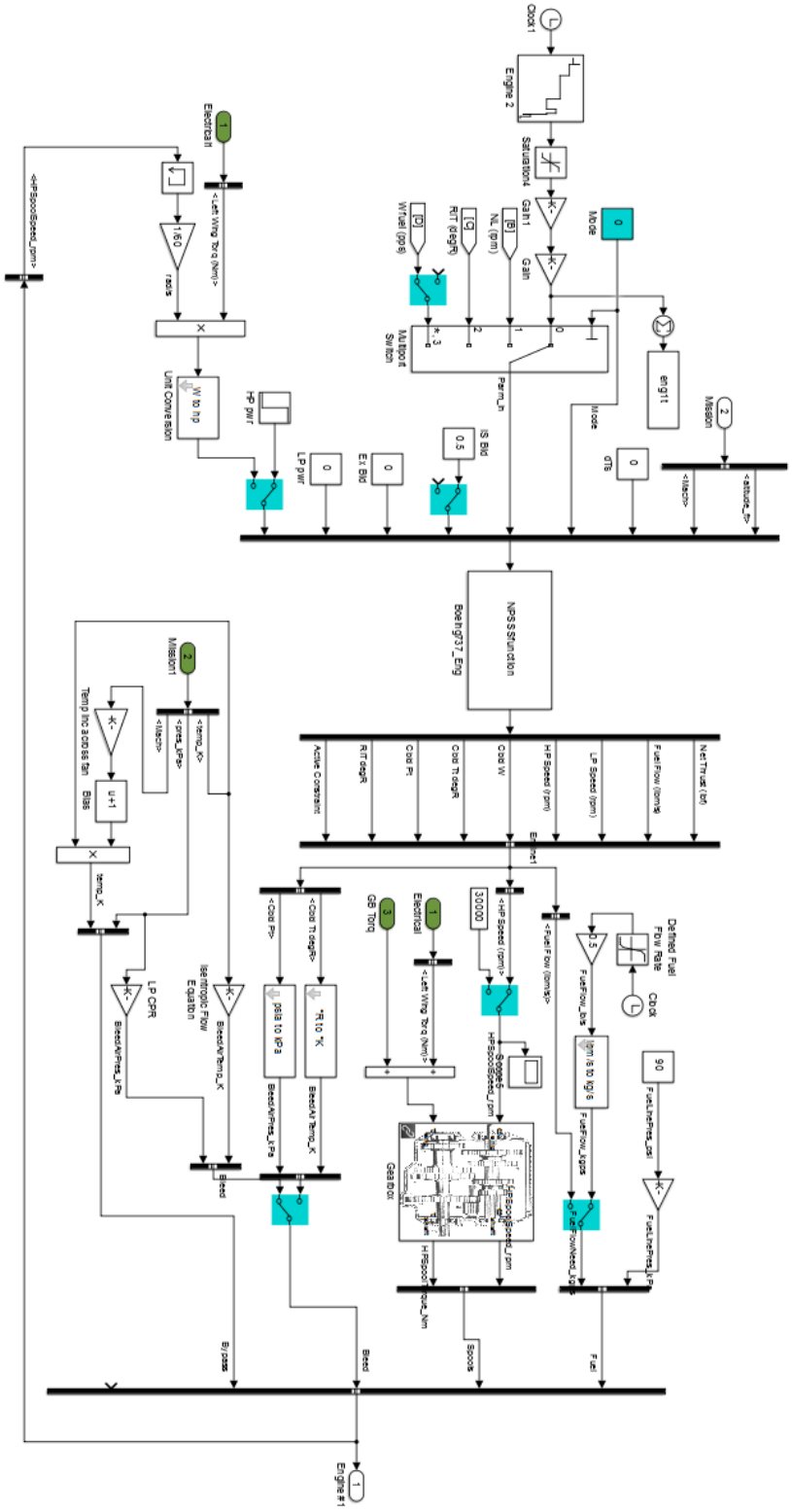

Figure 55: Simulink engine model with NPSS engine model

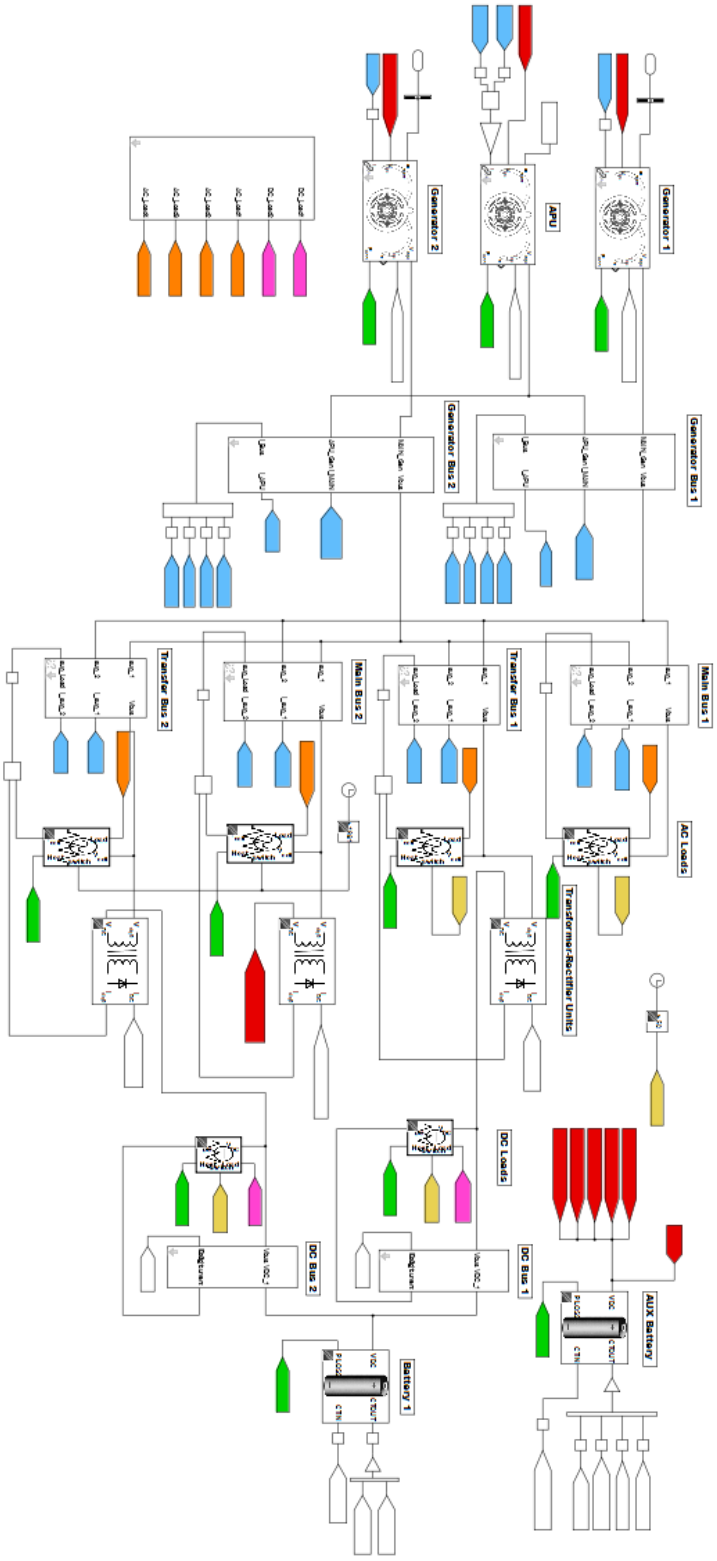

Figure 56: Simulink sample Boeing 737 model

APPENDIX B: GENERATOR INITIAL EQUATIONS

The following equations for the generator were taken from [14] and are the initial equations that solve several parameters for the generator. From the parameters detailed in the property menu of the generator seen in Figure 4, the per unit current and flux linkages are calculated by

$$I_d = \frac{-i_d}{I_{BDQ}} \qquad I_q = \frac{-i_q}{I_{BDQ}} \qquad I_0 = \frac{-i_0}{I_{BDQ}} \tag{36}$$

$$\psi_d = \frac{\lambda_d}{\Lambda_{BDQ}} \qquad \psi_q = \frac{\lambda_q}{\Lambda_{BDQ}} \qquad \psi_0 = \frac{\lambda_0}{\Lambda_{BDQ}} \tag{37}$$

where I_{BDQ} and Λ_{BDQ} are defined as

$$I_{BDQ} = \frac{2S_B}{3V_{BDQ}} \qquad \Lambda_{BDQ} = \frac{V_{BDQ}}{\omega_B} \qquad \nu = \frac{\omega}{\omega_B} \tag{38}$$

For Equations (3)-(9) several values need to be defined. The synchronous machine inductances are defined as

$$X_d = X_{ls} + X_{md}\,,\; X_q = X_{ls} + X_{mq} \tag{39}$$

$$X_{fd} = X_{lfd} + X_{md} \tag{40}$$

$$X'_d = X_d - \frac{X_{md}^2}{X_{fd}}\,,\; X'_q = X_q - \frac{X_{mq}^2}{X_{1q}} \tag{41}$$

$$X''_d = X_{ls} + \frac{1}{\frac{1}{X_{md}} + \frac{1}{X_{lfd}} + \frac{1}{X_{l1d}}}\,,\quad X''_q = X_{ls} + \frac{1}{\frac{1}{X_{mq}} + \frac{1}{X_{l1q}} + \frac{1}{X_{l2q}}} \tag{42}$$

The time constants are defined as

$$T'_{do} = \frac{X_{fd}}{w_s R_{fd}}\,,\; T'_{qo} = \frac{X_{1q}}{\omega_s R_{1q}} \tag{43}$$

$$T''_{do} = \frac{1}{\omega_s R_{1d}}\left(X_{l1d} + \frac{1}{\frac{1}{X_{md}} + \frac{1}{X_{lfd}}}\right),\; T''_{qo} = \frac{1}{\omega_s R_{2q}}\left(X_{l2q} + \frac{1}{\frac{1}{X_{mq}} + \frac{1}{X_{l1q}}}\right) \tag{44}$$

The field electromagnetic force is defined as

$$E_{fd} = \frac{X_{md}}{R_{fd}} \frac{v_{fd}}{S_B} I_{BDQ} \tag{45}$$

Once the voltages are calculated then their per-unit quantities are converted to actual units by using the following equations:

$$V_d = \frac{v_d}{V_{BDQ}} \qquad V_q = \frac{v_q}{V_{BDQ}} \qquad V_0 = \frac{v_0}{V_{BDQ}} \tag{46}$$

The torques are converted to actual units by

$$T_M = \frac{T_m}{T_B} \qquad T_{ELEC} = \frac{T_e}{T_B} \qquad T_{FW} = \frac{T_{fw}}{T_B} \tag{47}$$

where the base torque is given by

$$T_B = \frac{S_B}{\omega_B \frac{2}{P}} \tag{48}$$